2-f

X-622-69-537
PREPRINT

PROGRESSIVE SHOCK METAMORPHISM OF QUARTZITE EJECTA FROM THE SEDAN NUCLEAR EXPLOSION CRATER

NICHOLAS M. SHORT

DECEMBER 1969

GSFC
GODDARD SPACE FLIGHT CENTER
GREENBELT, MARYLAND

X-622-69-537

PROGRESSIVE SHOCK METAMORPHISM OF QUARTZITE EJECTA FROM THE SEDAN NUCLEAR EXPLOSION CRATER

Nicholas M. Short

December 1969

GODDARD SPACE FLIGHT CENTER
Greenbelt, Maryland

PROGRESSIVE SHOCK METAMORPHISM OF QUARTZITE EJECTA FROM THE SEDAN NUCLEAR EXPLOSION CRATER

Nicholas M. Short

NASA, Goddard Space Flight Center

Greenbelt, Maryland 20771

ABSTRACT

Cambrian and Mississipian orthoquartzites, present as fragments in alluvium, experienced shock-wave pressures up to 500+ kb during the SEDAN (100 kiloton) nuclear cratering explosion. Ejecta samples display diverse shock-damage effects correlative, in part, with increasing peak pressures, that establish a sequence of progressive shock metamorphism having these principal characteristics:

1. Lower pressure effects include cataclasis-like shattering of individual quartz grains by irregular microfractures and subparallel fractures cutting across grains.
2. Shock-induced discontinuities (planar features) in quartz show systematic variations with increasing shock damage. As planar feature sets per grain increase from 1.18 to 4.75, their orientations coincident with $\omega\{10\bar{1}3\}$ decrease in frequency from 60+% to 35% and $\xi\{11\bar{2}2\}$ sets decrease from 12% to 3%, whereas $\pi\{10\bar{1}2\}$ increase from 0% to 35%. Basal features, another shock criterion, form in relatively few samples. Examination by scanning electron microscope reveals planar features to

be structural discontinuities rather than open fractures. Lack of preferred orientation of quartz c-axes or of planar features relative to possible principal stress axes indicates that, at higher shock pressures, a nearly isotropic stress field was produced.

3. X-ray diffraction and asterism measurements demonstrate a progressive breakdown of crystal structure that increases directly with number and density of planar features.
4. Selective phase transformations, leading to disordered silica pseudomorphs (diaplectic glass or thetomorphs) are evident after planar features exceed ~ 4 sets/grain. X-ray diffraction and infrared absorption analyses confirm major structural breakdown at this stage.
5. The refractive indices of isotropized quartz range between 1.463 - 1.478 (except one coesite-bearing sample having an average index for quartz of 1.496) whereas that of iron-rich black glass in vesiculated quartzite ranges between 1.510 - 1.546.

Most shock effects produced by meteorite impact into quartzose crystalline rocks and sandstones are duplicated to varying degrees in the SEDAN quartzites.

CONTENTS

CONTENTS (Continued)

TABLES

INTRODUCTION

A meteorite impact origin has been proposed for almost 100 terrestrial crater-like structures ranging in diameter from a few tens of meters to more than 50 km (Freeberg, 1966). Characteristics common to most of these include circularity, breccia deposits filling a central depression, intense, localized structural deformation of the enclosing lithologic units, and, at some, unusual types of "volcanic" rocks. Depending on the degree of erosion, the surface expression of these structures grades from rimmed craters, sometimes with central uplifts, to morphologically indistinct astroblemes identified mainly from certain forms of structural disturbances and indications of shock metamorphism. Currently, evidence of metamorphic changes attributed to strong shock waves has been reported from over 50 of the possible impact structures. (Short and Bunch, 1968).

Definitive criteria for recognizing shock metamorphism are being developed from field and laboratory studies of both meteorite impact structures and nuclear explosion sites (Short, 1965, 1968a; French, 1968). Each type represents an event involving generation of shock pressures from tens of kilobars to more than a megabar and formation of the resulting structure on a time scale of a few seconds to several minutes. Over this pressure range, in which corresponding temperatures can rise above 1500° C, a regular sequence of progressive shock metamorphic effects is imposed on the rock media in which the event occurs (Chao, 1967, 1968; Dence, 1968; Engelhardt and Stöffler, 1968; Stöffler, 1965).

Experiments with controlled laboratory-scale explosions and projectile impacts place at least approximate values of peak shock pressures and associated temperatures on the observed effects (Ahrens and Rosenberg, 1968; Fryer, 1966; Hörz, 1968; Müller and Defourneaux, 1968; Short, 1968b; Wackerle, 1962).

The tectosilicates are the most useful recorders of shock effects in the various rock types present at known impact structures. Of these, quartz and other forms of SiO_2 are found at nearly all structures thus far investigated. Coesite and stishovite, the high pressure polymorphs of silica, occur naturally only at presumed impact sites. Shocked quartz also shows diagnostic fractures and lamellar microstructures or planar features that begin to develop near the Hugoniot elastic limit of 100-120 kb for single crystal quartz. Planar features continue to form as pressures rise to values at which diaplectic glass begins to develop.[1]

Robertson et al. (1968) have shown that, as shock damage to mineral grains increases, presumably in response to increasing pressure, the frequency

[1]The term "diaplectic" (from the Greek diaplesso, meaning to destroy by striking or beating) was introduced by Engelhardt and Stöffler (1968) during the 1966 Conference on Shock Metamorphism of Natural Materials. Applied as an adjective to a mineral name, diaplectic refers to the development of planar features, lamellae, and lowered refractive indices and birefringence by shock waves. Diaplectic glasses (derived from various minerals) are amorphous phases produced by a disordering or isotropization process, requiring shock wave action, in which once-crystalline grains preserve their prime morphological features (boundaries, cleavage, etc.) while undergoing a solid state transformation without melting. The term "thetomorphic" (adopted form) proposed by Chao (1967) at the same meeting has essentially the same meaning as diaplectic glass. This latter term is preferred in this paper to thetomorph because it connotes more specifically the breakdown or destruction of phases by shock waves known to have acted during the SEDAN explosion.

distribution of different rational crystallographic forms to which planar features can be related shifts systematically (Hörz, 1968; Engelhardt and Bertsch, 1969; Engelhardt and Stöffler, 1968). At lower pressures $\{10\bar{1}3\}$ is most abundant but, as pressures rise, such forms as $\{22\bar{4}1\}$ and $\{10\bar{1}2\}$ become relatively more common. The number of sets of different planar features and the density and spacing of these sets will also vary with the frequency distribution of orientations. Grades of progressive shock metamorphism of quartz-bearing rocks are assigned by Stöffler (1966), Engelhardt and Stöffler (1968) and Robertson et al. (1968) to particular field cases on the basis of stage or degree of microdeformation of quartz. Chao (1968) has devised a scale of increasing shock metamorphism defined by diagnostic changes observed in the silica minerals, feldspars, micas, amphiboles, etc. at shock pressures calibrated with respect to various effects in (co-associated) quartz that first appear at specific pressures attained during experiments to determine its Hugoniot curve.

Short (1965; 1968a) points out that most shock metamorphic effects imposed on rocks during impact are closely duplicated by nuclear explosions. A contained explosion in granodiorite (HARDHAT event; Short, 1966) produced irregular microfractures in both quartz and feldspars that increase in frequency within the inelastically stressed zone as the explosion center is approached. Planar features first appear in quartz at points calculated to have experienced pressures of about 100 kb. At the base of the HARDHAT explosion cavity, both quartz and feldspars were transformed to diaplectic glass at pressures exceeding 350 kb but

heat from a standing pool of shock-melted granodiorite caused extensive recrystallization of these isotropic phases.

Rocks from a second nuclear explosion have now been studied in detail. The SEDAN event of July, 1962 consisted of detonation of a 100 kiloton thermonuclear device at a depth of 194 m in the alluvial fill of the Yucca Flats structural basin at the A.E.C.'s Nevada Test Site (Echols, 1969) north of Las Vegas, Nevada. The shot depth, adjusted to yield and normalized to 1 kiloton, represents a scaled depth of burial of 53 m. The SEDAN crater has a maximum diameter of 402 m and an apparent depth of 110 m (Plate 1, A). In many respects it resembles the natural Barringer Meteor Crater in northeast Arizona (Plate 1, B) which has a rim diameter of 1300 m. A crater of this size could be produced in layered sandstones and carbonates at Meteor Crater by a 3.5 megaton nuclear explosion buried at the same scaled depth of burial as SEDAN (Short, 1965).

Streams and mass wasting have carried a variety of rock fragments of Cambrian to late Tertiary age from nearby hills into the basin containing the SEDAN crater. Such rocks, ranging from pea-sized fragments to boulders, were distributed as float in the alluvial fill encompassed by compressive shock waves, ranging in amplitude from tens of kilobars to a half megabar or more, that diverged from the explosion center during the early stages of cratering. As cratering proceeded, many fragments were ejected to fallback positions beyond the crater lip.

Although volcanic rock fragments and shock-melted alluvium predominate, about 10% of the ejecta consists of weakly metamorphosed Cambrian and

Mississippian quartz sandstones. Ninety-four specimens of these quartzites were collected from the throwout deposits around SEDAN. Thin sections cut from each specimen were examined petrographically for evidence of shock damage. Many specimens were also investigated by one or more instrumental methods including x-ray diffraction analysis, x-ray asterism, infrared absorption spectroscopy, electron microprobe analysis, scanning electron microscopy, thermoluminescence, and high temperature annealing. The results of these studies are reported in this paper. The primary objectives of the study are:

1. To describe in detail the modes of microdeformation of quartz shock during an explosion event of known characteristics and magnitude.
2. To compare and correlate the specific styles of shock damage observed in the SEDAN quartzites with the modes of deformation that characterize sandstone units at such impact structures as Meteor Crater, Arizona, Odessa, Texas, and Middlesboro, Kentucky in the United State, Carswell Lake in Canada, Aouelloul in Mauritania, Wabar in Arabia, and Gosses Bluff in Australia.
3. To relate the degrees of shock damage in quartz, as defined by petrographic criteria, to corresponding variations in properties determined by the several instrumental methods applied in this study, thus leading to other quantitative measures of progressive shock metamorphism.
4. To gain from these analyses a further understanding of the mechanisms by which quartz is altered when it is shock-loaded.

Because the initial position of any quartzite sample relative to the explosion center cannot be reconstructed simply from its location in the ejecta deposit, it is not possible to ascertain directly or by calculation the magnitude of peak pressure that acted on the sample. By reference to Chao's diagram (1968, Plate 1) of shock metamorphic changes as a function of pressure and temperature, together with other experimental data, the pressure interval within which certain observed effects are produced can be roughly estimated. As Chao states, the effects resulting from a given pressure will vary in different samples because of such diverse factors as grain size, porosity, sample size, duration of shock loading, wave interactions at free surfaces, rate of post-compression cooling, etc. It must be emphasized that the peak pressures assigned to the damage noted in the quartzites are therefore approximations whose limits of error cannot be numerically evaluated.

MEGASCOPIC PROPERTIES OF THE QUARTZITES

Two stratigraphic units outcropping as steeply-dipping, folded beds in the hills adjacent to Yucca Flats provide the quartzite fragments in the SEDAN alluvium. The upper Cambrian Stirling formation is exposed over a limited area about 1-3 km east of the SEDAN site. Unshocked fragments of this age are readily identified by their pinkish-brown color, uniform grain size, and strong cementation (Plate 2, A). Although the metamorphic grade is low, most Stirling lithologic units are usually described as metaquartzites because of their relative hardness and cohesion owing to recrystallization during burial and tectonic uplift.

The Mississippian Eleana formation is exposed over most of Quartzite Mountain and nearby hills some 6-7 km northwest of SEDAN. Eleana fragments are generally distinguished from Cambrian units by their various shades of darker brown, more variable grain sizes, and poorer sorting, higher proportions of clay and silt (grading into arenaceous siltstones), and more friable nature.

Weakly shocked Stirling and Eleana quartzite fragments show few outward signs of damage in hand specimens. At pressures above an estimated 100 kb, some samples of Eleana become more friable and lighter in color owing to increased microfracturing. Shock damage in the Stirling samples up to about 300 kb is even less obvious. Above this pressure, the large numbers of microfractures and planar features, usually visible with a hand lens, affect both Stirling and Eleana units. Typical samples show large reductions in specific gravity. Many become less cohesive and display decreased strength if rubbed or pulled.

Samples identified by microscope as diaplectic glasses are easily recognized in the field by their distinctive appearance (Plate 2, B). Although textures remain in tact, such specimens take on a glassy look. Some, representing more intensely shocked states, display visible "vesicles" and, in the extreme, resemble frothy pumice. Many fragments are cut by open fractures or gashes that penetrate inward from the surface. These wedge-shaped openings tend to follow pre-existing bedding planes or orient transversely at high angles to these planes. The fractures are similar to those observed in some specimens of shocked sandstone from Meteor Craters. Examined closely, the SEDAN samples

appear to have undergone volumetric expansion, with the openings acting as tapering tension cracks as the exterior enlarges. When held, such specimens seem very light in bulk density compared with unshocked fragments of equivalent dimensions. Under a hand lens, individual grains have a distinctly glassy appearance and those at exposed surfaces may have rounded edges or corners as though fused. The outsides of a few fragments show patches or blebs of a dark brownish-black, obsidian-like to vesicular glass.

PETROGRAPHIC CHARACTERISTICS OF THE SHOCKED QUARTZITES

In the following discussion of microscope observations, the order of presentation and accompanying photomicrograph illustrations are arranged according to the writer's assessment of progressive shock metamorphism of the Cambrian and Mississippian quartzites, usually without regard to stratigraphic identity.

A. Unshocked Quartzite: A texture typical of unshocked quartzite is shown in Plate 3, A. This sample was identified as Stirling formation by the presence around most grains of a thin coating of muscovite, derived by metamorphism of clay minerals that filled interstices in the original sediment. Nearly all interstices are now occupied by mica, small quartz fragments, and silica that bind the larger quartz grains into a cohesive state approaching that of metaquartzites. Many other samples are nearly free of mica. Quartz grains commonly interpenetrate; sometimes thin secondary silica overgrowths are formed. Feldspars

comprise from 5 to 10% of all grains. Feldspars are mostly albite-twinned plagioclase (An_{20} to An_{60}) and grid-twinned microcline, although some untwinned potash feldspar grains are recognized by the alteration products and optical figures. Heavy minerals are uncommon: apatite, sphene and rare zircons were noted.

These Cambrian quartzites, despite their tectonic history, contain relatively few microfractures. Some grains, however, are marked by well-formed deformation lamellae produced at the time of folding. In thin section, these normally appear as discontinuous, straight to curved, narrow linear features which show the familiar light-dark asymmetric pattern in both bright-field and phase contrast illumination (Carter, 1965). On average, less than one in twenty grains contain lamellae that usually occupy just a small fraction of the exposed areas. They occur mainly as single sets of parallel discontinuities that tend to orient along the same direction from grain to grain. More common are the linear to divergent zones of inclusions of mineral dust or fluids (in some thin sections these appear as diffuse bands).

Quartzite fragments shocked below about 300 kb commonly retain some distinctive evidence of their stratigraphic identity. Cambrian float at SEDAN is estimated to outnumber Mississippian samples by a two to one ratio.

B. Microfracturing and Other Effects of Weak Shock Pressures: Shock damage within grains is first indicated by development of a few fresh-looking, straight, curved, or zig-zagging fractures. Most individual fractures are generally up to

1/5 to 1/2 as long as the average lengths of their host grain. Many end abruptly at grain boundaries or against intersecting fractures. At the lowest levels of damage, the frequency or density of fractures per grain is not notably different from that observed in tectonically-stressed sandstones. Absence of any alteration products or concentration of mineral matter along the lines of break distinguishes these shock-induced cracks from the usually much older, mineralized microfractures in tectonites.

As shown by Short (1966a), the frequency of fracturing of quartz grains rises in proportion to the increase in peak shock pressures. In the SEDAN quartzites this generalization could not be verified directly because the samples cannot be accurately relocated in the original pressure field around the explosion center. Hence, the prime advantage in determining the Fracture Index (F.I.), a more quantitative evaluation of degree of microfracturing (Short, 1966a, p. 1206), is lost and this time-consuming measurement was not undertaken. For samples in which microfracturing is the only evident effect, the order of increasing shock damage was determined mainly by visual estimate of relative variations in fracture densities in equivalent areas within thin sections.

Plate 3, B exemplifies shock microfracturing developed to an extent seldom observed in tectonically-stressed rocks. Each grain is broken by numerous open cracks, the major ones extending over most of the grain length, which divide the grain into segments or slivers. In other samples, many small fractures abut against or branch off larger ones. Grains containing many short fractures

that break up the exposed area into irregular blocks are best described as shattered. In the more strongly fractured samples, individual grains can become so completely shattered that large segments are plucked out during thin section preparation. In many grains, parallelism of fracture sets reflects a crystallographic control of the planes of failure. The planes tend to orient along first-order rhomb, r $\{10\bar{1}1\}$, and, less comonly, the prism, m $\{10\bar{1}0\}$, faces and thus are a form of fracture cleavage.

Microfractures constitute the principal mode of failure up to pressures of 100 - 150 kb. Fractures superimposed on other types of shock damage continue to develop probably up to the stage at which diaplectic glass becomes common but they are decreasingly important as a means of strain release as planar features occupy more of each grain.

Quartz in most samples of unshocked SEDAN quartzites shows, in thin section, variable amounts of undulatory extinction or strain birefringence. Over much of the pressure range in which microfractures are the only sign of damage, this wavy extinction persists without obvious change in character or intensity. As the numbers of microfractures increase to the stage at which shattering dominates, new extinction effects are discernible. Most common are extinction patterns best described as "patchy" or "irregular wavy" which may coincide approximately with segments defined by fracture boundaries. These extinction patterns suggest that lattice strains cause the quartz crystal structure to separate into mosaics or blocks which experience small relative rotations throughout a grain.

Most SEDAN samples, from those which show only shattered quartz to those composed mainly of diaplectic glass, contain, in addition to microfractures, a small number of larger cracks extending from the surface generally across the specimen interior. The cracks invariably are filled with material identified as the silty alluvium that surrounded the quartzite fragments. As indicated by its birefringence, the alluvial material is still crystalline in samples containing only microfractures and a few planar features. Where planar features become the principal type of shock damage, and particularly where diaplectic glass is well-developed, these alluvium-filled veinlets are characterized by glass-like, brownish material identical to glass coatings on fragment surfaces. This glass is obviously shock-melted alluvial silt injected into the cracks early in the shock-loading stage (probably before ejection begins to separate fragments from alluvium). Water-rich alluvium converts to a quasi-melt (fluidizes) at pressures as low as 200 kb; somewhat higher pressures are needed as the water content drops. Thus, presence of alluvium glass in cracks within shocked quartzites serves as another guide to the peak pressures that altered the samples.

C. Planar Features in the Tectosilicates: Planar features[2] are probably the most general and useful criterion for recognizing the passage of shock waves

[2]Also termed planar elements or shock lamellae but incorrectly called deformation lamellae by some writers; for comprehensive discussions of planar feature properties and proposed mechanisms of formation, see papers by Carter, Chao, Dence, Engelhardt and Stöffler, Short, Hörz, Bunch, Robertson et al., Engelhardt et al., Sclar et al., and Bunch et al., in Shock Metamorphism of Natural Materials, Mono, 1968.

through rocks. These features appear to be discontinuities occupied by disordered phases of the host grains which result from distortion of atomic layers in the crystal structure in response to very high strain rates (p. 60). Planar features are known to form in minerals subjected to strong shocks but they have never been reported from tectonites or rocks involved in explosive eruptions of volcanic nature. In addition to quartz, planar features have been found by the writer in plagioclase and potash feldspars, enstatite, andalusite, pyrophyllite, kaolinite, hematite, and gypsum subjected to experimental shock loading to pressures in excess of 300 kb by the implosion tube method (Short, 1968b). Hörz (1968) has produced planar features in quartz at pressures as low as 100 - 150 kb, depending on crystal orientation, by impacting targets with projectiles fired from a powder gun. Müller and Defourneaux (1968), in explosives experiments on quartz, fix the first appearance of the $\{10\bar{1}3\}$ feature at 105 kb; $\{22\bar{4}1\}$ at 170 kb, and $\{10\bar{1}2\}$ at ~ 20 kb.

I. Quartz: Planar features in quartz are well-developed and often abundant in many SEDAN samples (Plate 3, C). In contrast to some planar features in quartz from rocks at many impact structures, those in the SEDAN quartzites are very sharp, fresh-looking, and free of the "decorations" caused by cavities, mineral matter, etc. which form along planar elements found in meteorite crater rocks. Absence of decorated SEDAN quartz planar features implies that the decoration process likely occurs over a prolonged period after an impact event, perhaps in response to solutions which permeate the breccia units. Decoration

is not simply a mechanical effect (such as pile-up of dislocation arrays) imposed at the time of shock lamellae formation, as some have proposed.

In weakly shocked samples planar features are limited to one to two sets per grain, localized over only about 10 - 25% of the exposed grain area. In sample (1067-65), planar features co-exist with a set of tectonic deformation lamellae. The latter are decorated by mineral inclusions whereas the shock-produced features are unmarked. The two types of discontinuities were also distinguished in phase contrast illumination by the bright-dark criterion suggested by Carter (1965) and show different orientations relative to the quartz-c-axes (p. 33).

With (inferred) increasing shock pressures, the numbers of individual planar features, the average number of sets per grain, the spacing of individuals and sets, the total area occupied by the features, and the distribution of both rational and irrational crystal plane orientations followed by the sets vary systematically (p. 26). For example, the grain shown in Plate 3, D contains several sets, oriented along the $\pi\{10\bar{1}2\}$ or d $\{01\bar{1}2\}$ planes, which begin to form at pressures about twice that needed to initiate the first appearance of $\omega\{10\bar{1}3\}$. The d or π sets can sometimes be differentiated from other sets by their close-spacing, slightly broader widths, wavy linearity, and prominent dark double borders around brighter interiors.

As the planar feature density approaches a maximum, at which the entire exposed surface area of each grain in thin section seems to be cut by contiguous individuals in multiple sets (Plate 4, A), the collective grains take on a diffuse

or "roughened" appearance in plane-polarized bright-field illumination (Plate 4, B). In cross-polarized light, these grains show reduced birefringence (δ = 0.006-0.001). Most grains assume low first-order grays which range within individuals from localized highlights of higher birefringence to near-to-complete darkness (isotropic) on stage rotation.

At higher magnifications (Plate 4, C), these planar features appear so tightly spaced as seemingly to preclude unaffected material remaining between individuals. The trace of an individual feature is about 0.5 microns in thickness but will seem wider (e.g., NNE set) if its plane lies at low angles to the plane of the thin section. When a polished and HE-etched surface cut through such a grain is examined at magnifications of 10,000 - 16,000x by electron microscopy (using platinum-shadowed carbon replicates), the planar features are revealed to be discontinuities as narrow as 0.05-0.10 microns lying between bands or blocks of apparently undisturbed and relatively less etched quartz (Plate 4, D) (Sclar, Short, and Cocks, 1968). The spacing of these thin discontinuities is irregularly variable. A series of discontinuities may be packed together with average separation of 0.1-0.3 microns and, in turn, this grouping may be 0.5 microns or more apart from the next close-spaced series. Where two sets of etched-out discontinuities cross each other, neither offsets nor bending of each set is evident. This implies that any slips or other movements along directions within the discontinuity planes are not visible at the magnifications reached. However, undetected slips of unit cell dimensions and their multiples, below the resolution

limit for these magnifications, cannot be ruled out in any explanation of the mechanism of planar feature genesis (p. 46).

Polished surfaces of several SEDAN samples were examined at magnifications up to 5000x in a Cambridge Stereoscan Electron Microscope. Plate 5 summarizes scanning observations made on one sample (767-3) which was HF-etched for different total times. In the unetched sample (A), planar features are not visible anywhere on the surfaces of grains which, in thin section, show abundant planar features. When etched only 5 seconds (in 48% HF), some planar features begin to stand out, (B); at higher magnification, (C), these are displayed as lighter bands which represent slight depressions that scatter the electron beam. After a 60 second etch, (D), additional sets are "developed" and the depressions widen and deepen to become actual openings or gaps. These results are interpreted to confirm the conclusion by Carter (1968), Engelhardt et al. (1968) and others that the planar features are <u>not</u> open fractures or linear voids (unless opened after formation by rarefaction waves, thin section preparation, etc.).

The effect of central brightness bounded on both sides by darker borders that characterizes a planar feature in bright-field illumination is a consequence of differences in refractive indices between the disordered phase within the discontinuity and the more crystalline phase separating adjacent discontinuities. This results in differential bending of light rays in a manner analogous to the Becke line effect. At the resolution limit of a petrographic microscope, the contributions from each narrow discontinuity in any series will be blended in, so

that the group acts as though it were a single discontinuity of greater average width.

II. Feldspars: Although feldspars comprise usually less than 10% of all grains in the SEDAN quartzites, in many samples some feldspars contain recognizable planar features. These are especially evident in twinned plagioclase and grid-twinned microcline. Potash feldspars seem less susceptible to planar feature development and more commonly fail by irregular fracturing, often forming distinctive patterns that resemble the trellis drainage patterns of stream systems. At higher shock pressures, the proportion of feldspar grains showing polysynthetic twins seems to decrease as the planar feature density of quartz increases. Thus, in sample 767-3, in which the quartz contains many close-spaced planar features and has reduced birefringence, twinning can be observed in a few feldspar grains only by carefully looking for it. In 1067-97, a sample already containing some diaplectic glass grains, visible twinning has become rare. Twins seem completely absent in samples having a high percentage of glass. These observations suggest that twinning in plagioclase and microcline may be relatively unstable under certain conditions of shock-loading, such that the twins disappear either by some undefined mechanism involving reversion to untwinned crystals or by selective transformation of twinned feldspars to diaplectic glass over a pressure range in which quartz is still crystalline.

Examples of planar features in SEDAN feldspars are shown in Plates 6 A and B. The grain appearing in Plate 6 A was identified as grid-twinned

microcline. At least five distinct sets of planar features develop within the albite and periclase twins but the crystallographic orientations of these sets was not determined.

An exceptional example of planar features in plagioclase (An_{45}) is depicted in Plate 6, B. At first glance, the pattern seems to resemble kink banding, similar in style to kinks developed in shocked micas. However, universal stage measurements demonstrate that the elongate bands containing en echelon sets of planar features are actually albite twins. Feldspars of nearly identical appearance have been described by Bunch (1968, Fig. 16) as mechanically twinned by shock. Many of the planar features are bent and a few, tiny, lensoid deformation bands have formed in some of the twins, indicating limited external rotations that led to kinking within the twins. Most of these planar features form sets that lie close to the (021) and (201) crystallographic planes.

Both the large numbers and resultant densities of planar features and the bending or distortion of twins in shocked feldspars from quartzites in which quartz shows less obvious damage indicate that the feldspar crystal structure is more readily deformed at the pressures acting on these samples. Feldspars depicted in Plate 6 are found in samples in which there are less than two planar features per quartz grain. The feldspar grain depicted in Plate 6, B occurs in a shattered quartzite devoid of planar features in quartz.

D. Diaplectic Glass: The grains shown in Plate 6, C and D represent a state transitional to that characterized by diaplectic glass. In cross-polarized light

the grains display greatly reduced birefringence (δ = 0.003-0.001). Most of the associated interstitial areas are now isotropic. This, plus the presence of tiny bubbles in the interstitial materials, suggests that some degree of localized melting has occurred in these areas. When the glassy grains are examined at higher magnifications, relicts or remnants of planar features can often be seen in some individuals (Plate 7, A). Those parts of the grains still occupied by planar features retain faint birefringence but areas devoid of these features are usually isotropic. The writer postulated elsewhere (Short, 1968b, p. 233) that diaplectic glass begins to form near pressures at which the density of the close-spaced planar features, representing zones of disordered material, reaches a saturation limit or maximum number per unit volume. Increasing shock pressures lead to further disordering until the crystal structure becomes so disorganized that all vestiges of planar features are removed.

With continuing increase in pressure, more grains are isotropized (total loss of birefingence) and interstitial areas show additional signs of conversion to melt-like material.[3] Outlines of pre-existing grains begin to take on unusual shapes, suggesting distortions of grains that behaved as though plastic or perhaps as highly viscous fluids. This behavior no doubt was momentary, occurring probably during the shock loading period and for a short time thereafter,

[3]If the interstitial fill contains mica, clay minerals, sulphides or carbonates, the shock pressures needed to "melt" this assemblage will be somewhat lower than those required to produce diaplectic glass or actual melting in quartz grains.

because evidence of extensive internal flow or fluid mixing is absent in the diaplectic glass. As peak shock pressures increase, corresponding post-compression temperatures of the individual grains reach higher values, accompanied by signs of localized flow within grains. Upon cooling, some diaplectic glass grains contract to produce fractures like those commonly noted in some true glasses that are rapidly quenched (Plate 7, B).

E. Vesiculation: With continued rise in shock pressures, vesiculation of the quartzites also increases. A microtexture typical of a very strongly shocked quartzite is depicted in Plate 7, C. Most of the larger tectosilicate grains retain their original shapes but now are completely converted to glass-like bodies. The interstitital fill or matrix and many included smaller grains are transformed to a state in which some fluidization can be assumed. Micas once present are no longer recognizable, except as occasional birefringent "highlights" where flakes are incompletely melted. At high magnifications, lines of flow in the interstitial glass are visible, especially where emphasized by brownish coloration, as streaks or smears which usually emanate from decomposed clay minerals and iron oxides. Ovoid bubbles or vesicles of varying sizes are distributed mainly throughout the vitrified matrix. These bubbles probably represent vaporization of adsorbed water and/or structural water within the micas (metamorphosed clays) in response to the subsequent temperature rises that result from the energy "deposited" as "waste heat" from the work of compression during shock wave passage. The possibility that some bubbles develop by

direct evaporation of the silicates at points (e.g., grain boundaries) where shock pressures were locally intense enough to produce this state (~600 kb for quartz), although difficult to prove, cannot be discounted.

At still greater shock pressures, vesiculation extends into the larger quartz grains. Most diaplectic glass shown in Plate 7, D contains dark, nondescript bands. These bands are here subparallel to one planar attitude but, more commonly, such bands are randomly oriented from grain to grain. At a higher magnification (Plate 8, A) these bands are resolved into small, coalesced bubbles within the glass whose surface now shows numerous, irregular and intersecting, tiny cracks or flaws typical of some stressed glasses. This coalescence of a linear array of bubbles is sometimes well-defined (Plate 8, B). The origin of these bubble bands was deduced from inspection of thin sections cut from unshocked samples. The distribution of the bands follows essentially the same patterns as those of lines or zones of mineral inclusions or bubble trains in the sedimentary quartz grains. The fluid content in these bubbles is changed to vapor by the post-compression temperature rise. This vapor expands against the host quartz which, for a brief time, remains sufficiently "fluidized" from the shock to allow the bubbles to grow within this viscous silica. Growth continues until the internal vapor pressure within each bubble cannot overcome the rapidly cooling silica that "stiffens" into diaplectic glass. The entire process probably requires only a fraction of a second at most.

F. Melting: Completely melted SEDAN quartzite samples were not found among the ejecta. The pumice-like specimens always retain some semblance of their original metasedimentary fabric, that is, the textural framework produced by the larger grains can still be recognized even though many individual grains have become distorted by highly localized internal flow. Perhaps the closest approach to melting is illustrated in Plate 8, C. In thin section, initial grain boundaries are now obscured. Vesicle diameters are larger than in most samples. The glassy walls between the bubbles show evidence of stretching but flow is still confined to the immediate region. In contrast to pumice texture, flow lines extending over distances of many bubble (or grain) diameters are absent, although elongation of some smaller bubbles may signify restricted flow on a small scale.

In several samples, patches of brownish-black glass appear in thin section as shown in Plate 8, D. This dark coloration is confined mainly to the interstitial areas. Qualitative analysis of the brownish glass, made by electron microprobe, indicates a sharp increase in iron content and some aluminum variation but no notable differences in silicon relative to the quartz grains. This sample probably came from the Mississippian units, many of which contain iron-rich mineral matter filling the pores. The fill presumably melts and remains fluid long enough for mixing and diffusion of Fe^{+3} to tint the resulting glass to various shades of brown. In bright transmitted light, at high magnification, these tinted glassy regions commonly show myriads of minute darker blotches of crystalline matter which may represent residues of decomposed minerals.

The early ejection and rapid cooling of fragments tossed out during cratering led to quick quenching of any phases within the quartzite that had actually melted. A much larger fraction of the alluvium in the inner region around the device experienced complete melting, aided by water and other fluxes. This alluvial melt remains hot and fluid long enough for distinctive flow patterns to result in parts of the glassy masses that make up the bulk of the lightweight SEDAN ejecta (Short, 1968a; Fig. 24). In principle, similarly transformed quartzite melt can be produced, but at much higher pressures and associated temperatures, and therefore in smaller quantities. No larger masses of quenched silica-rich melt, more or less homogenized by flow, have yet been found at SEDAN nor have silicate glass droplets been looked for in the fallback deposits. Further search for such a transformed quartzite is of interest to the problem of possible origin of tektites by shock melting of suitable materials.

According to Chao (1968; Fig. 1), at 400 kb the peak temperature generated from the compression wave is 640°C and the residual temperature after decompression is 610°C. Because this is well below the temperatures at which melting of silica should commence, the formation of diaplectic glass (thetomorphs) would seem to be primarily a mechanical (pressure-dependent) process. Approximately at 490 kb, formation of diaplectic glass gives way to actual melting. Compression and decompression temperatures associated with this pressure are about 1500°C and 1450°C respectively (extrapolated by the writer from Chao's Fig. 1). This second value is still below the dry fusion temperature of

1610°C needed to melt pure α-quartz crystals; pre-conditioning of crystal structures by shock presumably lowers the melting temperature. Chao estimates that vaporization of silica commences on a large scale at 600 kb (equivalent compression temperature of 2640°C) (see also Wackerle, 1962).

PETROGRAPHIC MEASUREMENTS ON SHOCKED QUARTZ GRAINS

A. Planar Features: The crystallographic orientations of planar features in SEDAN quartz have been established by plotting on a Schmidt equal-area steronet, the spatial positions of the quartz optic or c-axis and the pole or normal to each set of planar features in the same grain. As measured on the 4-axis universal stage, the observed orientations of sets are grouped into a frequency distribution of c-axis $\wedge$ $\perp$ planar features from 0° to 90°. The resulting histogram calls attention to the various possible rational crystal forms to which the planar features can be indexed. Those data bars on a histogram which fall within the error of measurement ($\sim \pm 6°$) around the angle characteristic of each form represent the percentage of planar features that are apparently coincident with (subparallel to) that form. Proof of coincidence requires a separate plotting operation (p. 28). Bars not near angles of forms of low index may indicate non-selective orientations, i.e., the features align along irrational planes.

I. Planar Features in Quartz: Six samples of shocked SEDAN quartzites, each containing planar features, were selected as control samples on which detailed orientation measurements were made. These samples cover the range

of variations noted by scanning all thin sections in which shock-induced lamellae are present. Thus, one end member represents the first appearance of these features and the other reflects the condition of maximum development before the stage in which the features start to disappear as grains become glassy.

Results of the measurements are summarized in Fig. 1. The sample sequence from upper left to lower right was preselected from visual assessment of shock damage while scanning the thin sections.

The total number of grains examined in any sample was fixed at 22 or multiples of 2 or 4 thereof. The ratio indicated for each sample marks the total number of planar sets measured in all grains divided by the total number of grains counted. The quotient represents the average number of planar feature sets per grain for that sample. The percentage value immediately below expresses the number of individuals in 100 grains surveyed by a systematic thin section traverse that contain visible planar features (after tilting the universal stage to look for hidden discontinuities). The number recorded along the 30° line is derived as follows: For interval x° the concentration index is defined as the ratio:

$$C.I = \frac{\text{number of poles in interval x}}{\text{total number of poles}} \times \frac{90°}{x°} .$$

The values given in each histogram are for the 15° interval between 16° and 30° and show the preponderance of poles lying in this interval. As the stereograms show, most of these poles can be assigned to the omega ($\omega\{10\bar{1}3\}$) form, whose

pole has an angle of about 23° to the c-axis, i.e., in the middle of the interval.

The trends indicated in the histogram sequence of Fig. 1 are well-defined. As shock damage (and, inferentially, shock pressure) rises, the average number of sets per grain also increase to a maximum near 5.[4] The number of grains which display planar sets also becomes greater until, at a ratio extrapolated to 4 sets per grain, every grain contains recognizable sets. Although not directly indicated numerically, the average set density increases and the spacing between individuals decreases as the number per grain of sets with different orientations increase.

At lower levels of shock damage, the concentration index clearly indicates $\omega\{10\bar{1}3\}$ to be the dominant crystal form controlling planar feature orientations. This form continues to be important over the entire sequence but other forms become relatively more frequent. Thus, a secondary maximum appears in the histograms of 1067-65 through A-19 at angles attributable either to r $\{10\bar{1}1\}$ (or its negative rhomb z $\{01\bar{1}1\}$) or $\xi\{11\bar{2}2\}$ or both. The pi feature, $\pi\{10\bar{1}2\}$, at 32-1/2° becomes increasingly more common through the sequence 767-6 - 1067-97. Expressed another way, through the six sample sequence up to maximum

[4]This is not the same as the maximum number noted in individual grains. In sample 1067-97, one grain contained 8 distinct sets having different orientations. One grain in 767-3 also had 8 sets and three other grains had 7. The largest number yet found in a SEDAN quartz grain is 10, in a sample not included in the histograms.

planar feature development, sets assumed coincident with ξ $\{10\bar{1}3\}$ decrease in relative frequency from 60 to 35%, ξ $\{11\bar{2}2\}$ sets decrease from 12 to 3%, and π $\{10\bar{1}2\}$ increases from 0 to 35%.

Robertson, Dence and Vos (1968) have recognized five progressive stages in development of planar features in quartz from Canadian craters. In their sequence, the following types of planar features first appear, as shock pressures increase, in this order: (1) Type A = c $\{0001\}$; (2) Type B = ω $\{10\bar{1}3\}$; (3) Type C = $\{22\bar{4}1\}$; (4) Type D = π $\{10\bar{1}2\}$, in grains with reduced biregringence; and (5) Type E = π $\{10\bar{1}2\}$, in grains with isotropic regions. Several types can co-exist in any sample but some one type will be most frequent. Applying this classification (appropriate to the shock pressure range between 100 - 400 kb) to the SEDAN quartzite samples appearing in Fig. 1, the sequence progresses from Type B (1067-65) through Type C (1067-63) to Type D (767-3) and then Type E (1067-97). No samples containing Type A features alone are known from the SEDAN collection. The Type C feature is never prominent in the SEDAN distribution, even though it persists along with x $\{51\bar{6}1\}$ through the Type E stage. The steady decrease in frequency of occurrence of ξ $\{11\bar{2}2\}$ with rising pressure makes it another useful indicator of progressive shock damage. Müller and Defourneaux (1968) find that the ξ feature first develops between 100 - 140 kb in association with the ω feature but doesn't form in significant numbers above $\sim$ 200 kb, even though ω continutes to occur in quartz subjected to 330 kb; this result is supported by the SEDAN data given in Fig. 1.

A histogram plot does not, of itself, establish the rational coincidence of any planar feature with a crystallographic form, even if c-axis - pole angles are coincident. To prove that planar features selectively orient along crystallographic lattice planes, the actual position of planar feature poles on a stereonet relative to symmetry positions of poles to all crystallographic planes of any form must be shown to coincide. Carter (1965) uses a known crystallographic plane (e.g., rhombohedral cleavage) to fix the a-axes after rotating the c-axis to the vertical on the net. If cleavage is poorly developed, the following procedure (suggested by M. Dence of the Dominion Observatory and used in a modified method by Engelhardt and Bertsch, 1969) can be substituted: The c-axis of each grain is rotated to the vertical from its initial position on the stereonet and associated planar features are moved through the same angular rotation along appropriate small circles. The resulting plot is then rotated as an overlay around the vertical axis until one or more poles of a particular form coincide with a symmetry pole for that form plotted on a stereogram base having its c-axis at the center. In actual practice, because the planar feature poles may not lie at the exact c-axis - $\perp$ pole angles, coincidence is accepted for whichever planar feature pole comes closest to a symmetry pole along one of the radials connecting symmetry points and net center. Once coincidence is arbitrarily chosen for one planar feature pole, all remaining poles are also fixed in various positions relative to symmetry poles. Many of these planar feature poles will lie close to other symmetry poles if there is real correspondence between planar feature orientations and crystallographic directions.

The faces of many hexagonal forms have both positive and negative orientations, so that there can be 6 possible symmetry pole positions for a form such as the rhombohedron. To obtain a more uniform distribution of planar feature poles on a combined stereonet plot, the writer rotates the coincidence pole for each new grain clockwise to the next successive 60° symmetry pole of a positive-negative form.

Although coincidence with any of the possible forms indicated on the histograms could be tested by this procedure, $\omega\{10\bar{1}3\}$ was chosen to illustrate the results because it normally is most frequent. Stereonet plots were made for all six samples of Fig. 1. A typical example, from sample 767-3, is presented in Fig. 2. The dashed lines are conical intersections which correspond to the histogram interval boundaries, at 16° and 30° as plotted in three-dimensional space projected on to the net. In all these plots, grains containing only one set within this interval are discarded, since this set is automatically fixed and offers no independent information about orientation. In Fig. 2, the set pole points lined up along radii containing the symmetry plane poles are the ones selected arbitrarily. Twenty-four grains having a total of 58 sets within the 16° - 30° interval were used to construct the plot. The 34 points not on the radii represent those whose orientations with respect to the other symmetry plane poles are to be determined.

Using ±6% as the maximum error for measurement of planar feature poles, 68% of these 34 points lie no further than 6° from the symmetry plane poles. If

instead, all 34 planar feature poles were to distribute randomly within the ring bounded by the 16° and 30° circles, then only 49% would fall within the 6° radial limit, expressed as an area around each symmetry plane pole. The percentage difference reflects the tendency for set poles to concentrate around the symmetry plane poles. Percentages ranging from 61 to 74% were obtained by making the same type of plot for the other five (Fig. 1) samples.[5] These results support the hypothesis that most planar features in the 16° - 30° interval actually orient parallel to $\omega\{10\bar{1}3\}$ planes. Some set poles lying outside the 6° area plot about midway between adjacent symmetry plane poles. These points may correspond to some other, as yet unidentified crystal form (possibly $\{11\bar{2}6\}$; M. Dence, pers. comm.).

Carter (1965) proposed that planar discontinuities oriented at or close to 0° are a criterion for the action of shock pressures on quartz inasmuch as deformation lamellae with basal orientations are usually rare in tectonites. He has observed basal discontinuities[6] by themselves or in association with omega and

[5]A maximum of 83% for co-association (within 6°) of planar feature poles with symmetry plane poles of all forms considered in quartz was determined by Engelhardt et al., (1968) from one Ries sample. Other Ries samples showed somewhat smaller percentages.

[6]Carter (1968) maintains that the discontinuities oriented along the (0001) plane develop through a mechanism similar to that by which deformation lamellae have been produced experimentally. He contends that these basal lamellae are distinguished from planar features by their bright-dark, asymmetric appearance in phase contrast illumination. Robertson et al., (1968) and Engelhardt and Bertsch (1969) do not accept this distinction between discontinuities in shocked quartz oriented parallel to the base and those of other orientations and have referred to the first type as basal features or planar features with basal orientation. These latter terms are used in this paper.

other planar features in quartz sandstones from Vredefort, Meteor Crater, and Middlesboro structures identified by other workers as possible impact craters. Similar planar features with basal orientation have been reported from the Ries Kessel in Bavaria and from at least 11 Canadian impact structures. In some samples, basal features constitute 10 to 50+% of the orientations identified.

A study of shocked rocks from over 30 impact structures has led the writer to conclude that planar features with basal orientation are much less common than omega, pi, and other planar feature orientations. This conclusion is supported by Robertson et al., (1968) who note that the basal orientation makes up usually less than 10% of all orientations determined for planar features present in strongly shocked quartz grains. Dence (1968) finds that c {0001} features (his Type A) predominate in Brent crater rocks only in a region of the rupture zone located below the crater base-breccia lens contact; within nearly all breccia fragments, basal features are decidedly subordinate. Because {0001} is generally the first (and sometimes only) planar feature type to appear in rocks showing only weak shock damage, this orientation is assumed to form primarily in the region enveloped by the expanding shock front within which the pressures are just above the Hugoniot elastic limit. Basal features fail to develop in quartz experimentally shocked by projectile impact (Hörz, 1968) or explosives lens detonation (Müller and Defourneaux, 1968).

Engelhardt et al., (1968, p. 477) provide a correction equation that adjusts for the effect of the 1 to 6 ratio of the basal form to those forms having six

potential symmetry planes available for determining the frequency distribution of planar feature orientations. For a typical distribution in quartz grains from a Ries sample, in which all planar features initially were equally weighted, application of the equation changes the frequency of basal features from 3% to 16%. Other samples, containing less than 10 basal features per hundred features measured, upon correction undergo frequency redistributions which, in some instances, indicate that, statistically, one-third or more of the orientations are basal, even though in actual numbers non-basal features outnumber those near 0° by an order of magnitude.

Basal features are rare in five of the six shocked SEDAN quartzites of Fig. 1, including 1067-65 which shows only a few planar features and hence is assumed to have experienced pressures just above the Hugoniot limit. In samples other than A-19, the histogram bars between 0° - 6° comprise no more than 2%. A-19, in contrast, shows a frequency of 15% for the 0° - 6° interval. After applying the correction derived by Engelhardt et al., (Eq. III, 1968, p. 477) to the frequency distributions shown in Fig. 1, the basal features show the following new percentages:

1067-65:	1%	767-6:	2%
1067-63:	8%	767-3:	5%
A-19:	51%	1067-97:	11%

Under the microscope, many of the planar features in A-19 are relatively faint until viewed in phase contrast illumination. Some of these same features appear

to have asymmetric bright-dark borders but the majority display the double dark borders characteristic of planar features, leaving unresolved the question of the distinction between basal (deformation) lamellae and planar features proposed by Carter (1965). These features are, however, shock-produced if, according to Carter, their basal orientation suffices to distinguish them from lamellae of tectonic origin.

The relatively large number of basal features in A-19, a sample apparently subjected to greater shock pressures than 1067-65 and 1067-63, seemingly weakens the argument that the basal orientation develops preferentially within the lowest pressure range at which any planar features first appear. The overall scarcity of basal features in most other samples supports the writer's contention that these discontinuities are statistically less useful than omega, pi, and other features as indicators of a shock origin. The fact that basal features occur in some shocked rocks, including SEDAN quartzites, requires that they be listed with other unusual and diagnostic planar feature orientations as valuable criteria for proving that shock waves have acted on rocks. Their relative importance should, nevertheless, be kept in proper perspective.

The histogram for 1067-65 has its maximum class interval between 16° - 18°, with a secondary maximum between 22° - 24°. Both pre-shock tectonic deformation lamellae and shock-induced planar features co-exist in this specimen (p. 14). Probably the majority of individuals in the 16° - 18° interval represents deformation lamellae which usually have their most frequent orientation within

or near this interval (Carter and Friedman, 1965). The frequency percent of this interval progressively decreases in the sequence of six samples in Fig. 1. Thus, the relative number of tectonic lamellae within the distributions diminishes are more shock-produced features are formed. If the contribution made by these lamellae is removed from the sets per grain ratio, the values for the less strongly shocked samples show considerable reductions. Also, the concentration index for sample 1067-65 and, to a lesser extent, 1067-63 is anomalously high because of the unseparated admixture of planar features and deformation lamellae.

B. Indices of Refraction: Refractive indices of quartz and its shocked derivatives were measured on grains from 16 SEDAN samples. The results are recorded in Table I in which samples are listed in the order of increasing shock damage, predetermined from thin section observations. Unshocked samples appear at the top and a vesiculated glassy sample indicative of intense shock damage is placed at the bottom. A summary of these data is as follows:

1. A slight decrease in ξ and ω is noted in the fractured (shattered) samples.
2. There is a somewhat greater drop in ξ and ω in grains containing moderate numbers of planar features but still retaining normal birefringence.
3. As the shock level corresponding to a planar feature sets per grain ratio near 4.50 is approached, the refractive indices undergo a large reduction, accompanied by a noticeable loss in birefringence (Plate 4,

Table I

Indices of Refraction

Sample Number	ω	ξ	Remarks
1067-96	1.545	1.551	Unshocked
A-2	1.544	1.553	Unshocked
1067-65	1.541	1.549	Few Planar Features
1067-63	1.540	1.549	Few Planar Features
A-19	1.541	1.549	Very few Planar Features
767-6	1.536	1.543	Moderate Planar Features
1067-47	1.539	1.547	Moderate Planar Features
1067-57	1.534	1.542	Many Planar Features
767-3	1.472	1.478	Abundant Planar Features
1067-97	1.468	1.472	Transition to Diaplectic Glass
1067-79	1.465	1.469	Partly Diaplectic Glass
A-17	1.465 ± 0.001		Largely Diaplectic Glass
A-17 (Black Glass)	1.510	1.546	Varies with Iron Content
A-6	1.463	1.474	Variable; Vesiculated
1067-41	1.478	1.482	Variable; Coesite-bearing
1067-88	1.464 ± 0.0005		Very Glassy

Measurements made in sodium light (λ = 5890 A) at 25° ± 2°C

Estimated accuracy of measurements: ±0.001

A and B). The inception of this drop occurs abruptly. Although the increase in sets per grain from 3.12 (767-6) to 4.53 (767-3) is not a significant jump, the drop in ξ from 1.543 to 1.478 is a major change. No samples yielded transitional index values between 1.530 and 1.496. This suggests that the crystal structure tends to become disordered over a relatively narrow range of pressures (p. 46).

4. Sample 1067-41 shows a greater range of indices than most others that contain some diaplectic glass or become vesiculated and pumice-like. In thin section, the grains display wider variation of birefringence than usual. This is the only SEDAN quartzite sample found to contain detectable coesite (p. 42). Some granular inclusions in the diaplectic quartz glass have indices near 1.59 and may be this mineral.

5. There is considerable index variation among grains from A-6, as well as 1067-97 and 1067-79. Although all three samples consist mainly of diaplectic glass, the grains vary in degree of isotropization as indicated by differences in birefringence.

6. The most strongly shocked samples (A-17, and 1067-88) contain many nearly isotropic grains with a single index of 1.463 - 1.465. Fused quartz has an index of 1.458(5) at 5892 A. The black glass present in A-17 is colored by varying amounts of iron, as indicated by electron microprobe analysis. The average index of the silica glass appears to increase with iron content, so that the highest index values correspond to the darkest glass.

C. Optic Axis Measurements: Sharp, centered and off-centered uniaxial optic axis figure are obtained from normally birefringent quartz grains containing planar features. As birefringence decreases in the transition to diaplectic glass, the isogyres of optic axis figures broaden and become diffuse. In the very strongly shocked sample 1067-97, those grains that still show weak birefringence produce anomalous biaxial figures (double isogyres which leave the field of view on rotation at least 20° greater than needed to eliminate uniaxial flash figures). The 2V estimated from these figures is around 10° - 20°. Biaxial figures were also noted in the few remaining birefringent quartz grains of several more intensely shocked samples.

D. Orientation of Principal Stress Axes: Sample 767-6 was selected to test the possible application to shocked rocks of two methods for locating the maximum (σ_1) and minimum (σ_3) principal stresses acting to deform a rock body. Although these methods are based on measurements of deformation lamellae, they should also apply to planar features if these result from lattice slips or shear displacements.

The "arrow" method devised by Christie and Raleigh (1957) consists of connecting the pole (marked by an arrowhead) to each set of deformation lamellae in a grain to the c-axis of that grain, as plotted on a stereonet, by an arc line along the appropriate great circle. If the arcs from all such grains form a girdle, the arrowheads tend to point towards a common center representing σ_1, the axis of compression. If no girdle results, σ_1 is assumed to lie in the region

of largest concentration of arc intersections. Carter and Friedman (1965) note that this method is valid mainly when lamellae are predominantly basal and that, for sub-basal (10° - 30°) lamellae, the arrows more frequently point to σ_3 (see also Heard and Carter, 1968).

Carter et al., (1964) found that the more deformed parts of grains with tectonic lamellae experienced larger rotations in the direction of compression. In their $c_2 - c_1$ method, the c-axis (c_2) measured in a part of a grain containing a greater density of lamellae is connected along a great circle arc to the c-axis (c_1) measured in another part showing fewer lamellae. The resulting arcs for many grains tend to converge towards the compression axis such that the majority of c_2 points lie closer to σ_1.

A plot of the arrow method results from measurements in 767-6 of 72 grains containing 93 ω sets appears in Fig. 3, B, along with overlays (A, C) used to isolate different aspects of the data. Inspection of these plots leads to these deductions: (1) there is no preferred orientation of c-axes (a slight maximum within the girdle in the northeast quadrant suggests monoclinic symmetry[7]); (2) the intersections of great circle arcs are somewhat more concentrated in this northeast quadrant, but there is no dominant clustering in any section of the girdle; (3) there is no prevailing direction towards which the arrows point; although not strictly random in orientation, the arrows tend to point in many

[7]Stereonet plots of c-axes show a triclinic symmetry for unshocked quartzite grains and a broad tendency towards monoclinic symmetry in samples shocked more strongly than 767-6.

non-convergent directions in any of the quadrants. It is concluded that the arrow method does not reveal either the σ_1 or σ_3 pole positions so that, in fact, there is no convincing evidence for discretely located principal stress axes in this sample.

Results of measurements of c_2 and c_1 axes in 30 carefully chosen grains from 767-6 are shown in Fig. 3, D. As in the arrow method results, there is no strong tendency for arc convergence or for c_2 poles to point consistently towards one region of the stereonet. Measurements from two other samples, containing smaller numbers of grains suited to the arrow and $c_2 - c_1$ methods, disclosed a similar absence of a distinct concentration of arcs pointing towards a possible σ_1 axis.

The proper interpretation of these results requires an appreciation of the state and duration of stresses operating as the shock waves pass through a sample. For progressively increasing peak shock pressures, stress differences within a series of shocked samples decrease until a quasi-isotropic stress field, in which $\sigma_1 = \sigma_2 = \sigma_3$, is attained in the more strongly shocked regions affected by the shock waves. This uniform stress state, during which the compressive waves cause a sudden, large decrease in volume, is referred to as hydrodynamic (in analogy to hydrostatic). At the shock level postulated for 767-6 ($\sim$ 200 kb), the internal stress field within that sample as a whole was approximately isotropic, although some departures from this state may have existed in and around individual grains. The near random and uniformly distributed arrow and $c_2 - c_1$

arcs are precisely the results expected from isotropic loading of the sample, thus making it impossible to locate any one stress axis or reconstruct the direction of maximum shock (compression) wave propagation. The diagrams in Fig. 3 therefore support the physical model of stress states in the high pressure zones around an underground nuclear explosion (Maenchen and Nuckolls, 1961).

Moreover, arrow and $c_2 - c_1$ diagrams obtained from tectonites or rock deformation experiments are appropriate to strain rates of $10^{-13} - 10^{-16}$ /sec (natural) and $10^{-3} - 10^{-8}$/sec (experimental) and to total load times that favor efficient deformation by external rotations and/or internal slip or glide. Shock waves, in contrast, deform rocks at rates of 10^{6}/sec - 10^{8}/sec and act for durations insufficient to facilitate the types of intracrystalline movements that characterize tectonic deformation. Thus, pronounced preferred orientation should not be expected in shocked rocks.

INSTRUMENTAL MEASUREMENTS

A. X-ray Diffraction: Twenty-three samples, chosen to span the entire spectrum of shock damage defined by petrographic observations, were examined by x-ray diffraction methods. Finely-ground powders mounted on glass slides with a Duco-acetone mix were x-rayed with Ni-filtered Cu Kα radiation in a General Electric XRD-5 diffraction spectrometer at goniometer and strip chart speeds of 2° 2θ/min. In several cases, film patterns were obtained from spindle-mounted samples in a Debye-Scherrer camera.

Typical x-ray spectrometer diffractograms for eight samples are shown in Fig. 4. The sequence from left to right is that of increasing shock damage ranging from an unshocked sample (A-2) through first appearance of diaplectic glass (A-5) to a vesiculated sample showing incipient melting (A-6). The steady decrease in relative peak heights of characteristic reflection planes for α-quartz at 2θ values of 20.7° (100), 26.6° (101), 36.5° (110), and 39.1° (102) is immediately apparent by inspection. Peaks at 28, 29, and 31 degrees are attributed to feldspars in several quartzite samples. Each peak height can be quantified by measuring its length (in cm) from the extrapolated baseline (background) in the immediate 2θ region of the peak to its tip. These measurements are presented in Table II.

Table II

X-ray Diffraction Peaks for Quartz[a]

Sample	2θ			Sample	2θ		
Number	36.5	26.6	20.7	Number	36.5	26.6	20.7
767-2	11.4	24+	14+	767-3	-	5.4	1.0
1067-63	8.0	22	13+	A	-	6.5	1.2
A-19	11.0	22+	14	767-5	-	5.8	1.4
767-1	1.8	18	5.9	A-8	-	1.0	-
767-6	5.6	18+	11.7	A-11	-	-	-*
1067-57	-	6.0	2.6	A-6	-	-	-*

*No distinct peaks; broad "hump" between 18 - 30° 2θ

[a]Peak heights (in cm) measured from tangent line to background lines

As the level of shock damage increases, the crystalline structure of the quartz undergoes progressive disorganization, as evidenced by the decreasing intensities of radiation reflected from the indicated planes. There is also a tendency for peak broadening to occur in samples such as 767-1 and 1067-57 which remain optically crystalline despite strong microfracturing. The successive disappearance of peaks closely follows the expectation based on relative strength or intensity of the major reflection planes in normal α-quartz. Thus, the (101) plane, with $I/I_1 = 100$, is identified in all patterns except A-6. The next strongest plane, (100), at a dA of 4.26 and relative intensity of 35, persists through A-5. Reflections from the (110) and (102) planes, with equivalent intensities of 12, disappear in patterns from samples shocked above the level of sample A.

Samples 767-1 and 1067-57 retain marked crystallinity, although quartz peaks for the latter are weaker, in accord with the greater density of planar features within its grains. Sample A, with an even higher density of planar features (4.65) and notable reduction in birefringence, shows still further loss in crystallinity. Samples A-5 and A-11 are characteristic of diaplectic glasses containing a few weakly birefringent grains. The surviving peak at 26.6° 2θ is presumably produced by such grains. The diffractograms for A-8 and especially A-6 are very similar to those made from glasses or highly disordered crystals. The broad "hump" between 18° and 30° 2θ is associated with silica-rich glasses.

Peaks characteristic of coesite (3.10 and 3.43 dA) and stishovite (2.96 and 1.53 dA) were looked for in every diffractogram. The two principal coesite

peaks were found in one sample, 1067-41, that produced no other peaks except a weak one at 26.6° 2θ for quartz. Detection of these coesite peaks normally requires a minimum of 5 - 10% (volume) of coesite in the (unconcentrated) bulk material. Grains with appropriate refractive indices for coesite were observed in this sample (p. 28). Six other samples from the sequence between A and A-6 were treated in HF by J. Fahey (U.S. Geological Survey) to obtain an insoluble residue which might contain coesite or stishovite. No evidence of these minerals in this concentrate was provided by x-ray diffraction.

B. X-ray Asterism: The extent to which the structure of a single crystal undergoes internal fragmentation and micro-displacements or rotations of the resulting mosaic "blocks" can be expressed at its degree of asterism (Guinier, 1952). Dachille, Meagher, and Vand (1964) were the first to use x-ray to assess shock damage in quartz. As a grain is shattered into increasing numbers of displaced domains, spots from characteristic reflection planes recorded on film during analysis of an unoriented, rotated single grain begin to elongate or spread. Ultimately, as more reflecting planes are rotated to new positions with increase in shattering and micro-deformation, the spots may coalesce to form rings analogous to those made by randomly oriented grains in mounts x-rayed by the Debye-Scherrer powder method. Dachille, Gigl, and Simons (1968) devised quantitative measures of asterism patterns in which, for a given radiation, the length (in mm) of individual spots or arcs for specified dA spacings defines the degree of asterism. Hörz (1969) has calibrated the degree of asterism as a

function of known peak pressures obtained from a series of shock experiments on selected minerals.

Asterism values were determined for quartz grains hand-picked from 14 SEDAN samples. Grains with maximum diameters of 1/2 - 2 mm, mounted on silica glass rods, were rotated at 1 rpm through a beam of Mo K α radiation in a 114.6 mm Norelco powder camera for 6 hours. The lengths of the most central diffraction spots for the 3.35 dA (12.15° 2θ) reflection plane of quartz were measured on the film but line breadths which did not show significant variation, were not determined. From 2 to 3 grains per sample were run and the line spreading values were then averaged.

Diffraction patterns obtained from six of these SEDAN samples appear in Plate 9. The spots from all reflecting planes display increasing lengths from sample 767-2 (unshocked) to A-6 (glassy). No noteworthy differences exist between 767-3 and 1067-65, a strongly fractured sample containing a few planar features. Spot coalescence becomes notable in A-19 and proceeds further in 767-6 and A-6. Sample A-8 gives no discernible lines; the resulting film pattern is equivalent to the diffractogram obtained from A-8, in which a broad, diffuse hump denotes the glassy state.

Asterism values determined for grains taken from the 6 samples used for planar feature measurements are placed in parentheses with the histograms of Fig. 1. The asterism values for two samples showing no optical evidence of shock deformation (767-2 and A-2) are 1.2 and 1.4. This slight spreading,

compared to values of 0.8 and 0.9 obtained for same-sized grains of quartz from St. Peter sandstone run as control, is attributed to the influence of tectonism on the Cambrian quartzites. Samples 1067-65 and 1067-63, each containing some planar features, show no significant increases in asterism. Asterism increases signficantly in grains from the remaining sample sequence through 1067-97. This correlates generally with increasing numbers and densities of planar feature sets. The planar features thus indirectly indicate fragmentation of individual grains into microaggregates which, in part, controls the degree of asterism in a deformed crystal. The isotropization process, which produces diaplectic glass, is first noticed in samples in which planar feature sets per grain reach values around 4.5 and asterism exceeds an estimated value of 7:0. Samples showing shock damage beyond that of 1067-97 will display x-ray asterism patterns like those of A-6 to A-8.

C. Thermoluminescence: The thermoluminescence of a series of unshocked and shocked SEDAN quartzite samples provided by the writer was determined by Dr. D. J. McDougall of Loyola College, Montreal, Canada. Dr. McDougall has kindly consented to publication of his results as a group of glow curves (Fig. 5). These show changes in peak intensity (in arbitrary units) of emitted light as sample powders are heated through the interval 60° - 120°C. The curves on the left result from replicate runs of the unshocked sample 767-2, using for each the particle size interval (in standard mesh units) as indicated. The curves displayed on the right represent runs made on the -60 + 120 mesh fraction of

the same unshocked sample and a group of shocked samples. The sample sequence, in terms of decreasing peak heights, is that of increasing shock damage, except for 1067-94 and A-13 which from petrographic evidence appear somewhat more shocked than 767-5.

The steady diminution in peak heights with decreasing particle sizes that characterize the unshocked sample runs may indicate that the overall surface area from which light is emitted is an important variable affecting the intensity. It is tempting to speculate that a somewhat analogous effect operates in the shocked samples, even though these were run at one uniform size.[8] The one obvious change progressing through the series of samples is the increasing number of deformation surfaces, first as microfractures and then as planar features. These may represent zones with notably different (lower) electron trap populations which cut down on the total emitted radiation or they may act to absorb internally emitted light (Fuex, unpubl. thesis, 1967).

An alternative explanation of the reduction in glow curve intensities may simply be that of temperature-induced discharge of electron traps. As shock pressures increase, the post-compression heating of samples will be more effective. Even moderately shocked samples (e.g., A-19) experience temperature rises of 50 - 100°C (plus an unknown contribution from heat transferred from

[8]Other factors to be considered are grinding effects which may introduce new traps, exposure of fresh surfaces that have low densities of pre-existing traps, and absorption of light within grains.

surroundings in the ejecta blanket); this would be sufficient to discharge some (pre-event) traps. More strongly shocked samples (e.g., 767-5 and 1067-44) would experience brief temperature rises of hundreds of degrees, enough to completely depopulate the traps.

Thus, the reduction of thermoluminescence in most of the shocked samples may have been caused either by production of zones in which traps are destroyed or reduced or by thermal drain effects. The increase of thermoluminescence in some samples may be the result of shock processes forcing electrons into metastable states.

D. Infrared Absorption: Absorption spectra within the wave length regions from 2.5 to 25 microns (4000 - 400 cm^{-1}) were obtained from 6 samples following an analysis procedure specified by Lyon (1967). Twenty mg. samples were mixed with 1.0 g IR grade KBr and pressed in a vacuum pelletizer into 1/2 inch pellets. Analysis was carried out on a Perkin-Elmer 621 IR Absorption Spectrophotometer. Results are given in Table III.

The band peak around 1080 cm^{-1} represents the SiO stretching mode of excitation, that at 460 cm^{-1} is an SiO bending mode, and that around 790 cm^{-1} is an Si bending mode. The peaks at 390 and 370 cm^{-1} are also due to quartz. Alpha quartz typically has absorption band peaks near 1093, 797, 694, 520, and 464 cm^{-1} and fused quartz at 1100, 800, and 470 cm^{-1}.

Bunch et al., (1968) report band peaks for disordered SEDAN quartzite at 1082, 795, 688, and 462 cm^{-1}. They note a small peak shift from 1095 cm^{-1} for

Table III

Infrared Absorption Peaks

Sample Number	Wave Number in cm^{-1} (Peak Height in cm)							
767-2	1078(9.0)	798(5.0)	778(5.2)	693(2.6)	515(3.0)	460(4.4)	393(2.0)	370(1.4)
1067-63	1072(8.5)	798(4.9)	780(5.1)	694(2.8)	514(2.9)	460(4.2)	395(2.0)	371(2.3)
767-6	1078(8.0)	795(4.5)	779(4.7)	692(1.9)	510(2.3)	459(4.4)	393(1.2)	370(1.4)
767-3	1080(9.4)	783(3.0)				460(4.9)	390(0.6)	370(0.7)
1067-79	1080(10.9)	790(4.0)				465(4.4)		
A-8	1085(10.8)	788(3.6)				463(4.5)		

α - quartz to 1082 cm^{-1} for the disordered phase. No such shift is evident in the present data.

The disappearance of bands at 795, 692, 510, 390, and 370 cm^{-1} in 767-3 is significant. Sample 767-6, which still shows these bands, contains numerous planar features (3.12 sets/grain) but retains near normal birefringence. As birefringence is lowered in 767-3, which contains 4.53 sets/grain, the fine structure in the absorption spectrum is lost. This suggests that structural damage, involving band distortions, begins to have an effect on the spectrum at about the same shock level that produces a notable increase in asterism, loss of secondary x-ray reflection plane intensities, and a visible drop in birefringence.

E. Annealing Experiments: Several samples of strongly shocked quartzites were heated for prolonged periods above 1000°C to learn whether this treatment removes or otherwise affects planar features. Unconfined cubes approximately 1.5 cm on a side were heated in air at a rate of 100°C/hr in a tube furnace. Three samples were raised to 1200°C ±20°C and a fourth to 1450°C ±30°C; these temperatures were maintained for 24 hours. After slow cooling, each sample was examined for changes by petrographic microscope and x-ray diffraction methods. The observed effects are summarized in Table IV.

A peculiar textural phenomenon (Plate 10, A) appears in the 767-5 sample heated to 1450°C, although similar features may be in an embryonic stage in the specimens annealed at lower temperatures. In less recrystallized grains,

Table IV

Effects of Annealing Experiments

	Sample Numbers			
	1067-94	1067-79	767-5	767-5
Initial State:	Diaplectic glass, with traces of planar features		Most quartz grains with weak birefringence; some, more or less diaplectic glass; many have planar features; interstices melted and vesiculated	
Maximum Temperatures °C:	1200°	1200°	1200°	1450°
Effect on Planar Features:	None re-appear		Planar features survive and appear sharper	Survive; masked by new phases
Changes in Birefringence:	No change		Restored to near normal (0.006 - 0.008)	(0.006 - 0.008)

Table IV (Continued)

	Sample Numbers			
	1067-94	1067-79	767-5	767-5
Melting Effects:	Some further melting in interstices		Increases in interstices, removing some vesicles through flow; glass develops brown tints	In interstices
X-ray Diffraction:	No restoration of crystallinity		Most major quartz peaks re-appear	No quartz peaks re-appear
New Phases:	None detected		Tridymite (in interstices?)	Cristobalite; now the major constituent
Recrystallization:	None		None	General in both grains and matrix (see Plate 10, A)

ovoid to arcuate microstructures of variable size develop in groups whose outlines superficially resemble overlapping reptile scales or bunches of grapes. The boundary of each microstructure is optically sharp. The markings are not cracks but appear to be growth surfaces which intersect or abut against optically continuous neighbors. Whole areas are subdivided by these spheroidal to polygonal bodies, some of which are confined to single grains whereas others extend across previous grain boundaries. Many of these bodies enclose patches of faint planar features. The markings persist even where recrystallization is extensive.

Similar bodies have been noted in intensely shocked granitic rock fragments from the Deep Bay, Canada structure (Plate 10, B) and, more recently, in granitic inclusions from injection veins at the Tenoumer, Mauritania structure. Their origin has heretofore been a mystery but the SEDAN annealing results now suggest that they are a form produced by recrystallization of glassy material at high temperatures. Ceramists have described polycrystalline textures derived by a process of secondary recrystallization or discontinuous grain growth (Kingery, 1960) in which preferential growth of larger bodies produces crystals having so many sides that boundaries appear to have distinct curvatures. In these, impurities or discontinuities can inhibit normal or continuous grain growth, so that boundaries with larger curvatures are favored because of their lower surface energies.

F. Summary of Instrumental Analyses: The data from these instrumental analyses generally confirm the sequence of shock damage established from petrographic measurements, as is evident in Table V. Samples listed in the column on the left are arranged in the order of increasing damage determined qualitatively by scanning the thin sections from these samples prior to either petrographic or instrumental analysis. In each remaining column, the order of damage as deduced by interpretation of the analytical results from the indicated method is shown by the numerical sequence in that column. In only a few cases are there any inversions in the order set up in the first column.

The chief conclusion reached from these instrumental analyses is that the several methods used are sensitive to even moderate changes in shock damage from sample to sample. X-ray diffraction and x-ray asterism, in particular, appear capable of quantitative discrimination of the degree of damage imposed. All methods indicate that the largest changes take place over the stages in which planar feature density approaches its maximum and diaplectic glass starts to form. However, the petrographic microscope still provides a greater amount of direct information than any of the instrumental methods applied in this study. Furthermore, coupling of measurements of the distribution, density, and orientation of planar features with instrumental data such as the x-ray asterism values (Fig. 1) leads to a coherent and consistent picture of the nature and extent of shock damage in quartz up to the stage at which diaplectic glass develops.

2

Table V

Summary of Measurements

Sample Number Arranged From Petrography		Planar Features Sets/ Grain	Indices of Refrac- tion	X-ray Diffrac- tion Analysis	X-ray Asterism	Infra- red	Thermo- Luminescence
1. A-2	Unshocked		1		2		
2. 1067-96	Unshocked		2				
3. 767-2	Unshocked			1	1	1	1
4. 1067-63	±100 kb	2	4	3	3	2	
5. 1067-65	±100 kb	1	3		4		
6. 767-1	±100 kb			5			
7. A-19	±200 kb	3	5	2	5		2
8. 767-6	±200 kb	4	6	4	6	3	
9. 1067-47	±200 kb		7				5
10. 1067-57	±300 kb		8	6			
11. 767-3	±300 kb	5	10	9	7	4	
12. A	±300 kb	6		7	8		
13. 767-5	±300 kb			8	10		6
14. 1067-97	±400 kb	7	11		9		
15. 1067-94	±400 kb						4
16. A-11	±400 kb			11	11		

ESTIMATED PEAK PRESSURE

Table V (Continued)

Sample Number Arranged From Petrography		Planar Features Sets/ Grain	Indices of Refraction	X-ray Diffraction Analysis	X-ray Asterism	Infrared	Thermoluminescence
17. 1067-79	±400 kb		12			5	
18. A-17			13				
19. A-8				10	12	6	
20. A-13							3
21. A-6	±500 kb		14	12	13		
22. 1067-41			9				
23. 1067-44							7
24. 1067-88			15				

ESTIMATED PEAK PRESSURE

DISCUSSION

In the introduction it was stated that many shock phenomena observed in the SEDAN quartzites duplicate, to a large extent, various aspects of shock metamorphism found in quartz sandstones collected from meteorite craters. There are, however, some important differences which must be evaluated before the results of the SEDAN study can be used to interpret shock effects in the sandstones—and quartz-bearing rocks in general—at impact sites. Several major differences are made immediately evident by comparing the characteristics

shown in Table VI for SEDAN with those from 12 impact structures at which shocked sandstones are present (adapted from Table I of Short and Bunch, 1968).[9]

A distinct pattern emerges from this comparison: namely, the extent and character of shock damage in the sandstones described from the majority of these impact structures is not as varied as in SEDAN quartzites. Impacted quartz-rich sandstones seem to react to shock pressures mainly by first fracturing and crushing, then, in some cases, converting to diaplectic glass, and, finally, for several structures, melting to impactites. In most of these sandstones, planar features are usually poorly developed or even absent in recovered samples. This observation may, in part, reflect sampling factors: at some structures, samples have not yet been obtained from the central fill whereas at others this fill is now removed by erosion.

But, the fundamental reason for this difference in behavior, if indeed it is real, lies in the generally higher porosities of most sandstones compared with the tightly cemented SEDAN-type quartzites. During the earlier stages of shock compression, grains will tend to break and fragment as they are pushed into existing voids. The porosity must be sharply reduced, so that the grains are tightly compacted, before any residual compression acts to produce planar features. In effect, porous materials over much of the target volume affected

[9]Photomicrographs illustrating shock features in sandstones from most of these structures appear in Short and Bunch (1968), Bunch and Cohen (1964), Chao (1967, 1968), Cook (1968), Currie (1968), and French (1968).

Table VI

Shock Effects in Sandstones from Explosion and Impact Craters

Characteristics	SEDAN	Meteor Crater Ariz.	Odessa Craters Texas	Sierra Madera Texas	Decaturville Mo.	Kentland Ind.	Middlesboro Kent.	Carswell Lake Canada	Bosumtwi Cr. Ghana	Vredefort S. Afr.	Wabar Craters Arabia	Henbury Craters Austral.	Gosses Bluff Austral.
Initial Porosity	Low	Moderate	Moderate	Low to Moderate	Moderate	Moderate (?)	Low to Moderate	Moderate	Low to Moderate	Low	High	Moderate to High	Low to Moderate
Planar Features	Wide Range	Some; Not Common	Not Present	A Few	Not Present	Not Present	Some; Limited Orient.	Not Present	Some; Not Common	Basal & Omega Types	Not Present	Present	Basal & Omega
Diaplectic Glass	Common	Common	None	None	None	None	None	None	Some	None	Some (?)	Some	Some (?)
Melting & Vesiculation	Rare	Common	None	None	None	None	None	None	Common	None	Common	None	Some
Vesiculation	Common	Common	None	None	None	None	None	None	Some	None	Common	None	None
Remarks:		A		B	B		A	C		C	D		

A: Planar Features usually not well-developed and many may be a form of tight cleavage

B: Planar Features have been noted in "floating" quartz grains, etc. in carbonate units

C: Planar Features are well-developed in the granitic rocks in the central crater "floor"

D: Present uncertainty as to presence of "true" planar features; may be cleavage only

None: In some entries, none means not observed to date rather than not produced.

by shock waves should experience only crushing and shattering. Pressures may decay to levels insufficient to develop planar features by the time grains have been compressed to a volume equivalent to compact crystalline materials. The SEDAN quartzites, in contrast, were initially tightly cemented so that they responded to shock more like granite than typical sandstones and therefore display the wider diversity of shock damage characteristic of crystalline rocks. Only in the lower porosity quartzites from Vredefort, and, to a lesser extent, in sandstones from Bosumtwi, Henbury and Gosses Bluff do multiple sets of planar features develop with the range of orientations and densities observed in the more strongly shocked SEDAN samples.

Although high porosities may prevent extensive planar feature development, they are directly responsible for the relative ease with which the sandstones undergo varying degrees of fusion ending with melted target rock (impactites). Wackerle (1962), Ahrens and Gregson (1964), and others have pointed out that shock loading of porous rocks converts a much greater fraction of work done in compression directly to heat than is the case for denser, low porosity rocks. Thus at a given peak pressure, there should be a greater likelihood of melting of porous rocks than of dense rocks of the same mineral composition owing to the higher post-compression temperatures developed from the "waste heat." Again, the relative "tightness" of the SEDAN quartzites may account for the apparent absence of melted ejecta comparable to some of the sandstone impactites.

This view is supported by the implosion tube experiments devised by Short (1968b). When loose quartz sand was packed in the tube, implosion resulted in shock-lithification (Short, 1966b) that produced a coherent, tight sandstone from the porous mixture. Microscope analysis indicates that deformation is accomplished by fragmentation, with smaller pieces, broken loose from fractured grains, being shoved into closing interstices. Because of the increased likelihood of melting in shock-compressed porous rocks, the central (axial) region of some implosion tube samples is completely melted. Only a few planar features were formed in the larger grains, although peak pressures momentarily exceeded 400 kb. In well-cemented sandstone cores imploded in like manner, the planar feature density per grain was still relatively low but was consistently greater than in imploded loose grains. Stress concentrations at grain contacts are probably an important factor in developing planar features in closely interlocked sandstones and in forming fractures instead in loosely packed sand (or porous sandstone). The experiments suggest also that load time during the compression stage (in this case, less than 30 microseconds) is also a factor in determining the extent to which planar features develop. Extrapolating this idea to impacted sandstones, the lower proportion of the total target rocks containing planar features could mean that much of the load time in compression is spent in crushing the porous sandstones to a compacted state required for effective formation of these features. An obvious test of this hypothesis would be to measure porosities in unshocked equivalents of the same impacted units, and make a more

extensive search for planar features in samples collected from different zones in each structure.

It appears, then, that the SEDAN quartzites behave more like some crystalline rocks than like sandstones having high porosities. Engelhardt and Bertsch (1969) report two significant findings, quite similar to results presented in this paper, from their studies of quartz in Ries crystalline breccias. First, they note (cf., their Table VIII) that the decrease in indices of refraction of progressively shocked quartz is not continuous but shows a missing interval or discontinuity between about 1.53 and 1.49. This is the same range of index values established as absent in quartz from the shocked SEDAN quartzites. As they remark, their sample sequence covering this range does not show any abnormal increments in planar feature density. Thus, there is only a moderate increase in planar features in samples containing diaplectic glass grains ($\overline{\eta} = \sim 1.49$), as compared to samples with still crystalline quartz ($\eta_\alpha > 1.53$). Second, the variations they determined for frequency distributions of several common planar feature orientations broadly follow the same sequential changes shown by the quartzite samples of Fig. 1.

The exact nature and precise mechanism of formation of the highly distinctive planar features, suggested by many workers (e.g., Carter, 1968b) as definitive proof of meteoritic impact, are not yet fully understood. Studies by Chao (1967) and by Engelhardt et al., (1968), supported by examination in the Leitz interference microscope, indicate the planar discontinuities to be composed

of material which usually has lower refractive indices than the more crystalline material between discontinuities. A single-valued index approaching that of glass, equivalent in composition to the host grains, has been obtained from measurements of specific shock lamellae but there is some spread of values for sets within and between grains and between samples shocked at different pressures. Engelhardt and Bertsch (1969) and Hörz (pers. comm.) have proposed that this disordered material was, at the moment of formation, a high pressure phase (coesite, stishovite, or a mixture of these) which transforms on pressure release to a silica glass.[10]

The discontinuities thus appear to be disordered phases of the same composition as the host materials but disagreement continues as to whether this disordering develops by some slip mechanism involving bending, glide, or rupture of the lattice in some planar direction, or crushing that causes random bond-bending and -breaking in a zone defined by the discontinuity, or some

[10]This hypothesis has not been supported by actual identification of crystalline phases within lamellae. Engelhardt and Bertsch describe the material filling planar lamellae in quartz from selected stishovite-bearing samples of Ries granite as having a higher refractive index but they admit that identification of this material as stishovite is an assumption. Chao (1968) states that optimum shock pressure ranges for formation of metastable stishovite and coesite are 380-400 and 400-420kb. respectively but notes that these phases can begin to form under shock conditions at much lower pressures (~150kb for stishovite). If this 400 ± 20kb value is a critical one for production and stability of the high pressure silica phases, then they should not survive, or even form, in the 100-400kb pressure range over which planar features develop. Diaplectic glass first appears at pressures near 400kb, so that association of coesite and/or stishovite with the early stages of isotropization is expected. The one SEDAN sample containing significant amounts of coesite fits this requirement; only a few of its grains are essentially diaplectic glass.

unspecified thermo-mechanical process. Most workers now believe that the planar features form during the early or compressive-loading phase immediately after the abrupt change of state involving volume decrease associated with the jump condition that marks the passage of the shock front through the material.

The possibility that temperature plays an important role in producing planar features needs further exploration. At 100 - 150 kb, the post-compression temperature is only 100 - 150°C whereas in the interval marked by maximum development of planar features the residual temperatures reach 300 - 600°C (Chao, 1968). Although the discontinuity planes probably are localized during compression, any partial isotropization of materials within them may commence or intensify during unloading when the effects of temperature rise accompanying volume expansion can implement the disordering process. It is even conceivable that planar features only start to form in the decompression stage when grains are momentarily in a quasi-plastic state affected by the higher temperatures.

The report by Heard and Carter (1968), who examined the influence of strength, strain rate, and temperature on development of deformation lamellae in quartz bears on the above viewpoint. These workers found that the flow mechanism deduced for lamellae formation begins with cataclasis and then changes to basal through sub-basal (10° - 30°) to non-selective slip as temperatures rise. This is essentially the sequence constructed from the study of the shocked SEDAN quartzites, in which temperatures rise in direct proportion to pressure increases. Heard and Carter also demonstrated that, at higher strain rates,

the temperatures required to initiate a specific slip orientation also must rise. Thus, at 10^{-3}/sec the transition between basal and sub-basal slip takes place at 850°C—temperatures much higher than the 100+°C calculated to operate as omega features first appear in shocked quartz. Whether, at the very high strain rates associated with shock wave passage, the effect of the moderate rises in temperature (in a non-equilibrium process) will be sufficient to influence planar feature development is, at this time, an open question.

Baeta and Ashbee (1967) and K. Currie of the Canadian Geological Survey (pers. comm.) have produced planar feature-like discontinuities in quartz and feldspar respectively by plastic deformation that results when crystals are strained at compressions rates of the order 10^{-4}/sec in an unconfined loading system in which temperatures are varied up to 900°C. These investigators have not reported the orientations of these discontinuities nor have they confirmed the presence of glassy phases within the planar zones. The writer suspects that these discontinuities are a type of lamellae similar to those formed in Heard and Carter's experiments.

SUMMARY

Quartzites, subjected to a wide range of transient stress states during the SEDAN crater-forming nuclear explosion, experience essentially all primary phases of shock metamorphism known to result from a meteorite impact event. At peak shock pressures up to ~ 100 kb, quartz grains deform mainly by irregular micro-fracturing and cleaving on a scale rarely observed in tectonites.

Planar features first appear in association with these fractures between 100 - 150 kb (estimated). The planar discontinuities, consisting of disordered silica layers aligned in crystallographically-controlled directions, develop in increasing numbers, density, and diversity of orientations as peak pressures acting at different distances from the explosion center rise to values above 300 kb. Within the interval of 100 - 300+ kb, the most common orientation followed by planar features is $\omega\{10\bar{1}3\}$ but with increasing pressures its relative abundance diminishes with the appearance of features oriented close to symmetry planes of the $\pi\{10\bar{1}2\}$, $\xi\{11\bar{2}2\}$, and $\{22\bar{4}1\}$ forms. At pressures probably in excess of 350 - 400 kb, the average density of planar features within a grain reaches its maximum ($\sim$ 5 sets/grain) and the quartz crystal structure, already disordered along the discontinuities, becomes more or less completely isotropized so that the grain takes on a "glassy" look while retaining its original shape. Melting first commences within the matrix materials, some of which contain water that aids in the fusion process. As pressures increase to levels above 400 kb, quartz grains begin to melt and flow internally. This effect may result, in part, from the bond-breaking action of shock waves but is largely influenced by the high post-compression temperatures associated with these pressures. Extreme melting to form impactite-like glasses did not occur. Thermally-activated recrystallization of isotropized grains, commonly observed in rocks from the breccia lens in impact structures, is absent in SEDAN samples but was produced artificially in several samples used in annealing experiments.

Distortions of crystal structure, ranging from mechanical displacement of micro-domains through slips and ruptures at the unit cell scale to bending or breaking of atomic bonds can be detected by x-ray diffraction, x-ray asterism, infrared, electron microscope, and thermoluminescence analyses. Most of these methods distinguish differences in the degree of shock damage between samples; in one respect, this sensitivity merely reflects the wide response range possible in a shocked crystalline substance subjected to pressures from a few tens of kilobars to a half megabar. Various measurements, both instrumental and petrographic, all point to a major change of state in quartz after its conversion to diaplectic glass.

When compared with porous quartz sandstones from certain meteorite impact structures, the SEDAN quartzites have many shock effects in common but also show better development of planar features formed over the pressure interval in which impacted sandstones at some structures fail primarily by fracturing, crushing, or partial melting. This difference in behavior is explained by the relative "tightness" or low porosity characteristic of the SEDAN quartzites and well-cemented sandstones from some impact structures. SEDAN quartz also responds more like quartz in granites, gneisses, and other crystalline rocks in that planar features follow the same sequence of orientations when shocked over equivalent pressure intervals.

REFERENCES

Ahrens, T. J. and V. G. Gregson, Shock compression of crustal rocks: data for quartz, calcite, and plagioclase rocks, J. Geophys. Res., v. 69, 4839-4874 (1964)

Ahrens, T. J. and J. T. Rosenberg, Shock metamorphism: experiments on quartz and plagioclase, in French, B. M. and Short, N. M., eds., Shock Metamorphism of Natural Materials, Baltimore, Mono Press, 59-81 (1963)

Baeta, R. D. and K. H. G. Ashbee, Plastic deformation and fracture of quartz at atmospheric pressure, Phil. Mag., v. 14, 931-938 (1967)

Bunch, T. E., Some characteristics of selected minerals from craters, in French, B. M. and Short, N. M. Shock Metamorphism of Natural Materials, Baltimore, Mono Press, 413-432 (1968)

Bunch, T. E., and A. J. Cohen, Shock deformation of quartz from two meteorite craters: Geol. Soc. America Bull, v. 75, 1263-1266 (1964)

Bunch, T. E., A. J. Cohen and M. R. Dence, Shock-induced structural disorder in plagioclase and quartz: in French, B. M. and Short, N. M., Shock Metamorphism of Natural Materials, Baltimore, Mono Press, 509-518 (1968)

Carter, N. L., Basal quartz deformation lamellae - a criterion for recognition of impactites: Am. Jour. Sci., v. 263, 786-806 (1965)

_____, Dynamic deformation of quartz: in French, B. M. and Short, N. M., Shock Metamorphism of Natural Materials, Baltimore, Mono Press, 453-474 (1968a)

Carter, N. L., Meteoritic impact and deformation of quartz, Science, v. 160, 526-528 (1968b)

Carter, N. L. and M. Friedman, Dynamic analysis of deformed quartz and calcite from the Dry Creek Ridge Anticline, Montana: Am. Jour. Sci., v. 263, 747-785 (1965)

Carter, N. L., J. M. Christie and D. T. Griggs, Experimental deformation and recrystallization of quartz: Jour. Geology, v. 72, 687-733 (1964)

Chao, E. C. T., Impact metamorphism: in Abelson, P. H., Researches in Geochemistry, v. 2, New York, John Wiley & Sons, Inc., 204-233 (1967)

_____, Pressure and Temperature histories of impact metamorphosed rocks - based on petrographic observations: in French, B. M. and Short, N. M., Shock Metamorphism of Natural Materials, Baltimore, Mono Press, 135-158 (1968)

Christie, J. M. and C. B. Raleigh, The origin of deformation lamellae in quartz; Am. Jour. Sci., v. 257, 385-407 (1959)

Cook, P. J., The Gosses Bluff cryptoexplosion structure; Jour. Geology, v. 76, 123-139 (1968)

Currie, K. L., A note on shock metamorphism in the Carswell Circular Structure, Saskatchewan: in French, B. M. and Short, N. M., Shock Metamorphism of Natural Materials, Baltimore, Mono Press, 379-382 (1968)

Dachille, F., E. P. Meagher and V. Vand, Shock-induced polymorphism or alteration in minerals (abs): Geol. Soc. Am. Spec. Paper 82, 40 (1964)

Dachille, F., P. Gigl and P. Y. Simons, Experimental and analytical studies of crystalline damage useful for the recognition of impact structures: in French, B. M. and Short, N. M., eds., Shock Metamorphism of Natural Materials, Baltimore, Mono Press, 555-569 (1968)

Dence, M. R., Shock zoning at Canadian craters: Petrography and structural implications: in French, B. M. and Short, N. M., eds., Shock Metamorphism of Natural Materials, Baltimore, Mono Press, 169-184 (1968)

Emmons, R. C., The universal stage: Geol. Soc. Am. Memoir 8, 205 (1943)

Engelhardt, W. V., F. Hörz, D. Stöffler and W. Bertsch, Observations on quartz deformation in the breccias of West Clearwater Lake, Canada, and the Ries Basin, Germany: in French, B. M. and Short, N. M., eds., Shock Metamorphism of Natural Materials, Baltimore, Mono Press, 475-482 (1968)

Engelhardt, W. V. and D. Stöffler, Stages of shock metamorphism in the crystalline rocks of the Ries Basin, Germany: in French, B. M. and Short, N. M., eds., Shock Metamorphism of Natural Materials, Baltimore, Mono Press, 159-168 (1968)

Engelhardt, W. V. and W. Bertsch, Shock Induced Planar Deformation Structures in Quartz from the Ries Crater, Germany, Contributions to Mineral. & Petrol., v. 20, 203-234 (1969)

Freeberg, J. H., Terrestrial impact structures - a bibliography; U.S. Geol. Survey Bull. 1220, 91 (1966)

French, B. M., Shock metamorphism as a geological process: in French, B. M. and Short, N. M., eds., Shock Metamorphism of Natural Materials, Baltimore, Mono Press, 1-17 (1968)

Fryer, C. C., Shock deformation of quartz sand: Internat. Jour. Rock Mech. and Min. Sci., v. 3, 81-88 (1966)

Fuex, A. N., Thermoluminescence of shocked granodiorite: unpubl. thesis, Univ. of Houston, Texas (1967)

Guinier, A., X-ray Crystallographic Technology: London, Hilger and Watts, Ltd., 330 (1952)

Heard, H. C. and N. L. Carter, Experimentally induced "natural" intragranular flow in quartz and quartzite; Am. Jour. Sci., v. 266, 1-42 (1968)

Hörz, F., Statistical measurements of deformation structures and refractive indices in experimentally shock loaded quartz: in French, B. M. and Short, N. M., eds., Shock Metamorphism of Natural Materials, Baltimore, Mono Press, 243-254 (1968)

Kingery, W. D., Introduction to Ceramics, New York, John Wiley & Sons, Inc., 781 (1960)

Lyon, R. J. P., Infrared Absorption Spectroscopy, Ch. 8: in Physical Methods in Determinative Mineralogy, J. Zussman, ed., London, Academic Press, 371-404 (1967)

Maenchen, G. and J. H. Nuckolls, Calculation of Underground Explosions: Lawrence Radiation Laboratory, Livermore, Calif., Rept., UCRL-6438, Pt. II, J1-6 (1961)

Müller, W. F. V. and Defourneaux, M., Deformationsstrukturen in Quarz als Indikator fur Stosswellen: Eine experimentelle Untersuchung an Quarz-Einkristallen: Zeit. fur Geophysik, v. 34, 483-504 (1968)

Robertson, P. B., M. R. Dence and M. A. Vos, Deformation in rock-forming minerals from Canadian craters: in French, B. M. and Short, N. M., eds., Shock Metamorphism of Natural Materials, Baltimore, Mono Press, 433-452 (1968)

Sclar, C. B., N. M. Short and G. C. Cocks, Shock-wave damage in quartz as revealed by electron and incident-light microscopy: in French, B. M. and Short, N. M., eds., Shock Metamorphism of Natural Materials, Baltimore, Mono Press, 483-492 (1968)

Shoemaker, E. M., Impact mechanics at Meteor Crater, Arizona; in Middlehurst, B. M. and Kuiper, G. P., The Solar System, v. 4: The Moon, Meteorites, and Comets, Chicago, Univ. of Chicago Press, 301-336 (1963)

Short, N. M., A Comparison of features characteristic of nuclear explosion craters and astroblemes: Annals N. Y. Acad. Sci., v. 123, 573-616 (1965)

_____, Effects of shock pressures from a nuclear explosion on mechanical and optical properties of granodiorite: Jour. Geophys. Res., v. 71, 1195-1215 (1966)

_____, Shock-lithification of unconsolidated materials: Science, v. 154, 382-384 (1966b)

_____, Petrographic evidence for an impact origin of the West Hawk Lake structure, Manitoba, Canada (abs): Trans. Am. Geophys. Union, v. 48, 147 (1967)

Short, N. M., Nuclear-explosion-induced microdeformation of rocks: an aid to the recognition of meteorite impact structures: in French, B. M. and Short, N. M., eds., Shock Metamorphism of Natural Materials, Baltimore, Mono Press, 185-210 (1968a)

_____, Experimental microdeformation of rock materials by shock pressures from laboratory-scale impacts and explosions: in French, B. M. and Short, N. M., eds., Shock Metamorphism of Natural Materials, Baltimore, Mono Press, 219-242 (1968b)

Short, N. M. and T. E. Bunch, A worldwide inventory of features characteristic of rocks associated with presumed meteorite impact craters: in French, B. M. and Short, N. M., eds., Shock Metamorphism of Natural Materials, Baltimore, Mono Press, 267-284 (1968)

Slemmons, D. B., Determination of volcanic and plutonic plagioclases using a three- or four-axis universal stage; Geol. Soc. Amer. Spec. Paper 69, 64 p. (1962)

Stöffler, D., Deformation and Umwandlung von Plagioklas durch Stosswellen in den Gesteinen des Nordlinger Ries: Contr. Mineral. and Petrol., v. 16, 51-83 (1967)

Wackerle, J., Shock-wave compression of quartz: Jour. Appl. Physics, v. 33, 922-937 (1961)

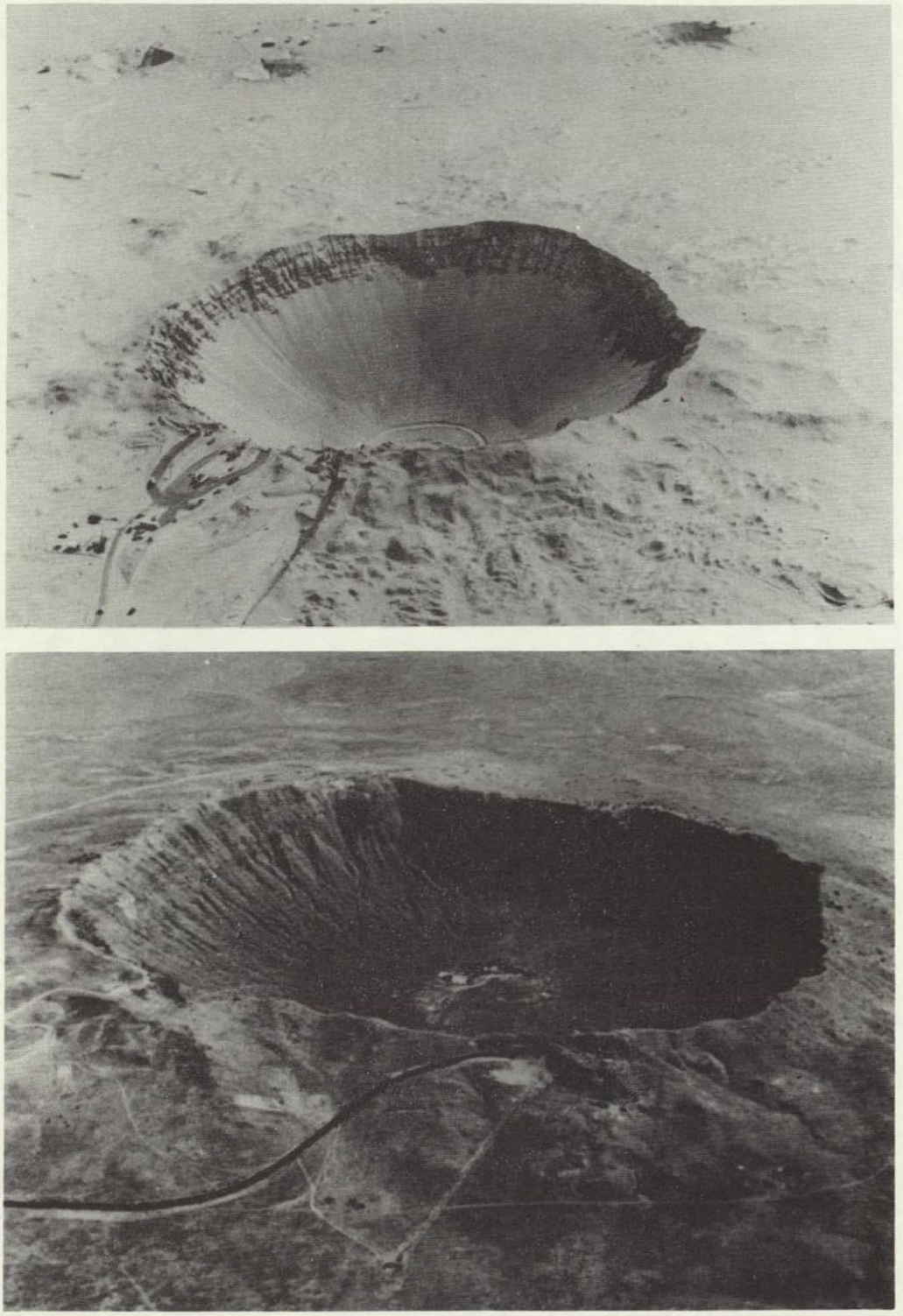

Plate 1. Upper photo shows the SEDAN nuclear crater resulting from detonation of 100-kiloton nuclear device in an alluvial basin at the Nevada Test Site in the western U.S.; crater is about 350 meters wide. Lower photo presents for comparison the 1300 meter diameter Meteor crater in Arizona, formed by impact into flat-lying sandstones and carbonates.

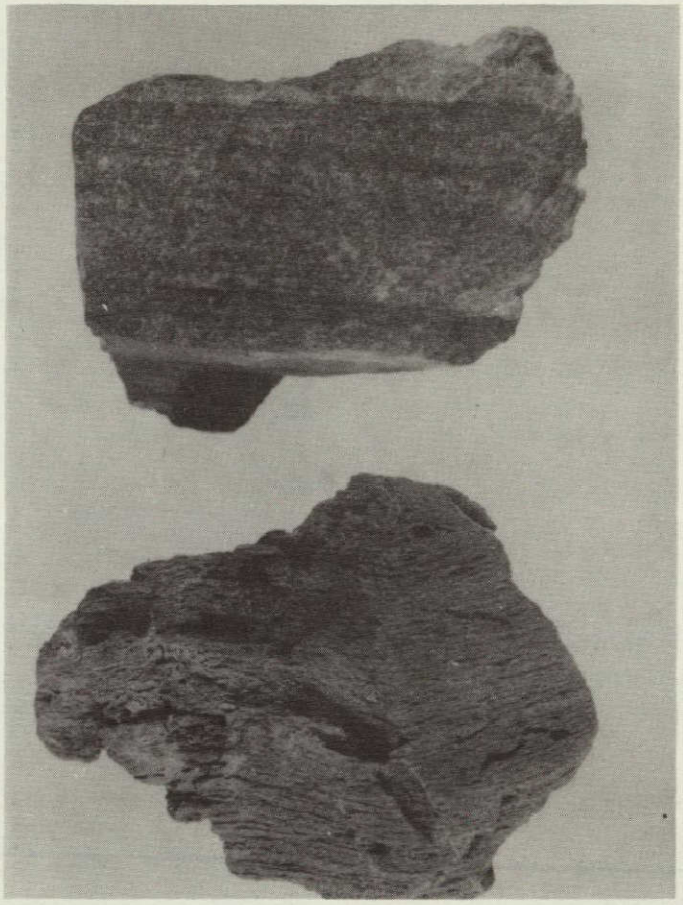

Plate 2. Upper sample is an unshocked float fragment of Stirling quartzite showing color-banded deposition layers, tight cementation, and absence of fractures. Lower sample is an intensely shocked fragment of Stirling quartzite, now converted to a "glassy" state while preserving the textural fabric. Specific gravity of sample is 1.2. Open gashes are caused by shock-induced preferential expansion along pre-existing bedding planes; sample is vesiculated on a hand-lens scale.

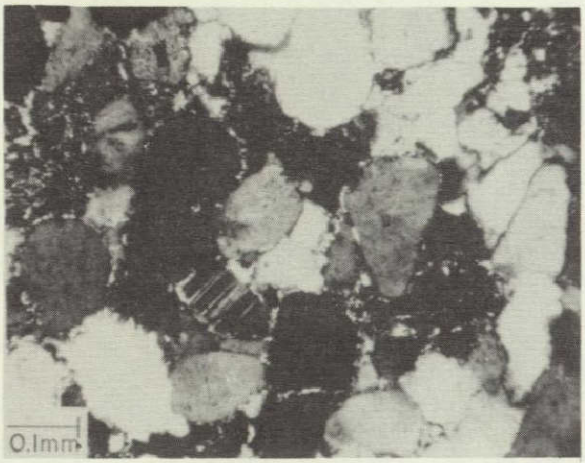

Plate 3(a). Unshocked Cambrian quartzite. Quartz grains are tightly packed; muscovite surrounds many grains. Twinned feldspar makes up about 10% of the grains. Sample 1067-96. All photomicrographs in these figures are taken with nicols crossed unless otherwise stated.

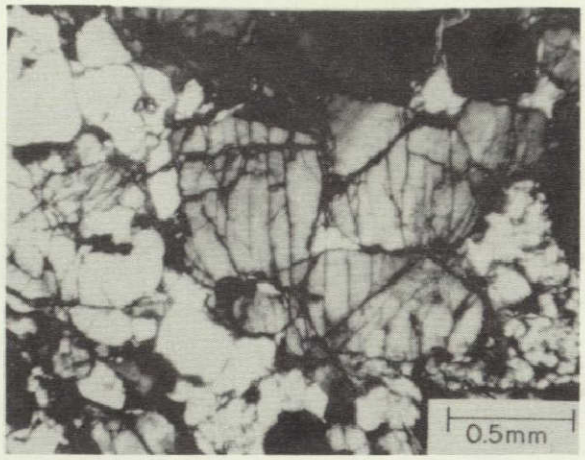

Plate 3(b). Strongly fractured sample 1067-65; many fractures tend to follow cleavage directions.

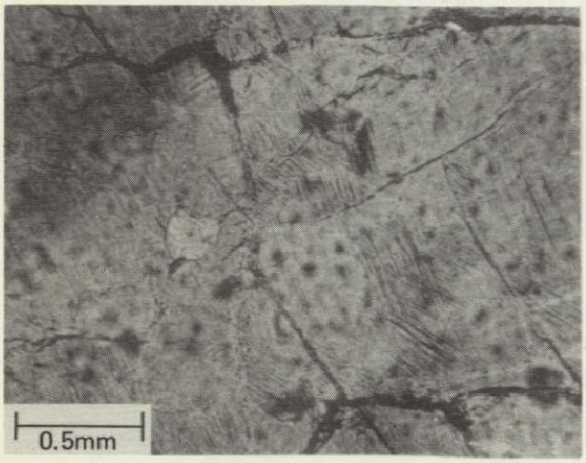

Plate 3(c). Several quartz grains in a Cambrian quartzite sample (767-6), visible in transmitted light with nicols uncrossed, containing two well-defined sets (NW and NNW) of planar features; a weak third set runs E-W. Small grain in left center is apatite.

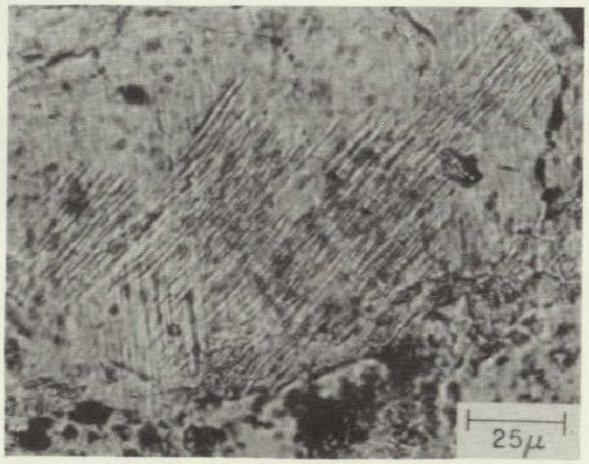

Plate 3(d). N-S and NE sets of close-spaced, broad, and wavy planar features in 767-1, which orient along planes following the $\pi\{10\bar{1}2\}$ crystal form.

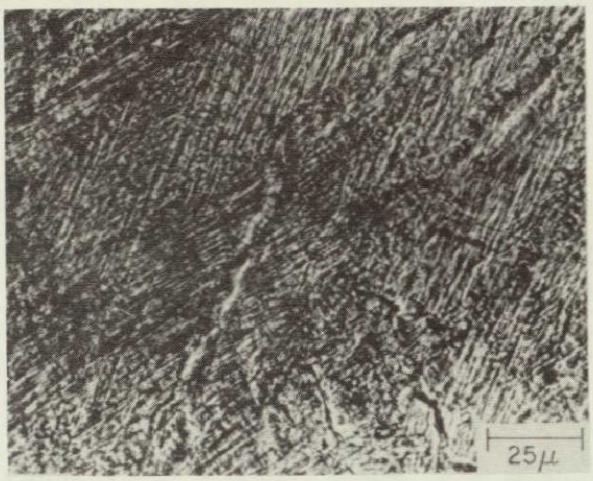

Plate 4(a). A single grain in sample A, with two close-spaced sets of planar features (NNE and NE) and two faint sets (E-W and NW); the number of sets per grain approaches a maximum in this sample.

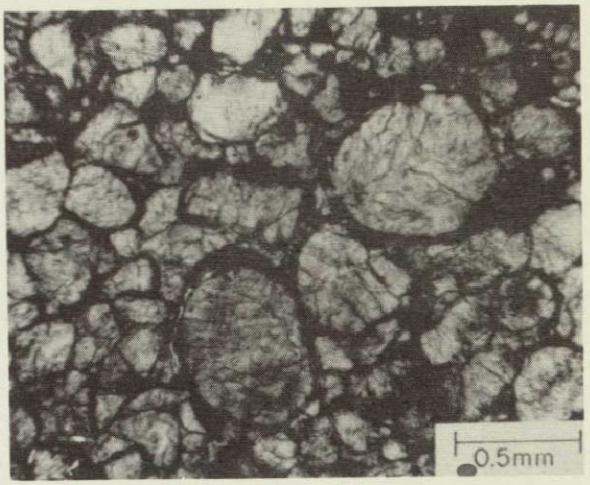

Plate 4(b). Low magnification view of the textural character of sample A, seen here with Nicols uncrossed. The grains, completely criss-crossed with planar features, cause the transmitted light to appear diffuse. Dark material between the grains is presumably "melted" iron-rich matrix.

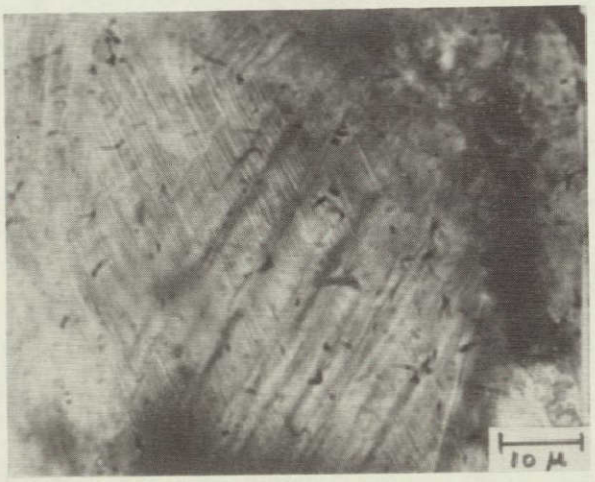

Plate 4(c). NW and NE sets of planar features, photographed at 1000x. The NW set is close-spaced whereas the more widely spaced NE set is broader and more poorly defined because of its low angle orientation relative to the thin section plane. 767-3.

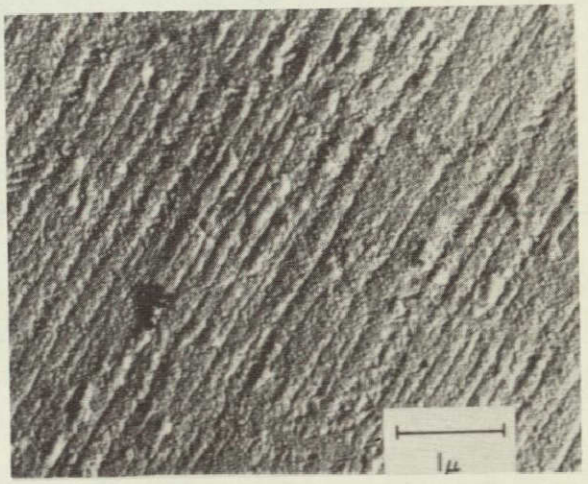

Plate 4(d). Photomicrograph taken from an illuminated platinum-shadowed carbon replicate at a magnification near 14000x in the electron microscope. The NE-trending discontinuities are thin, individual planar features etched out with HF. Sample A. Photo courtesy C.B. Sclar.

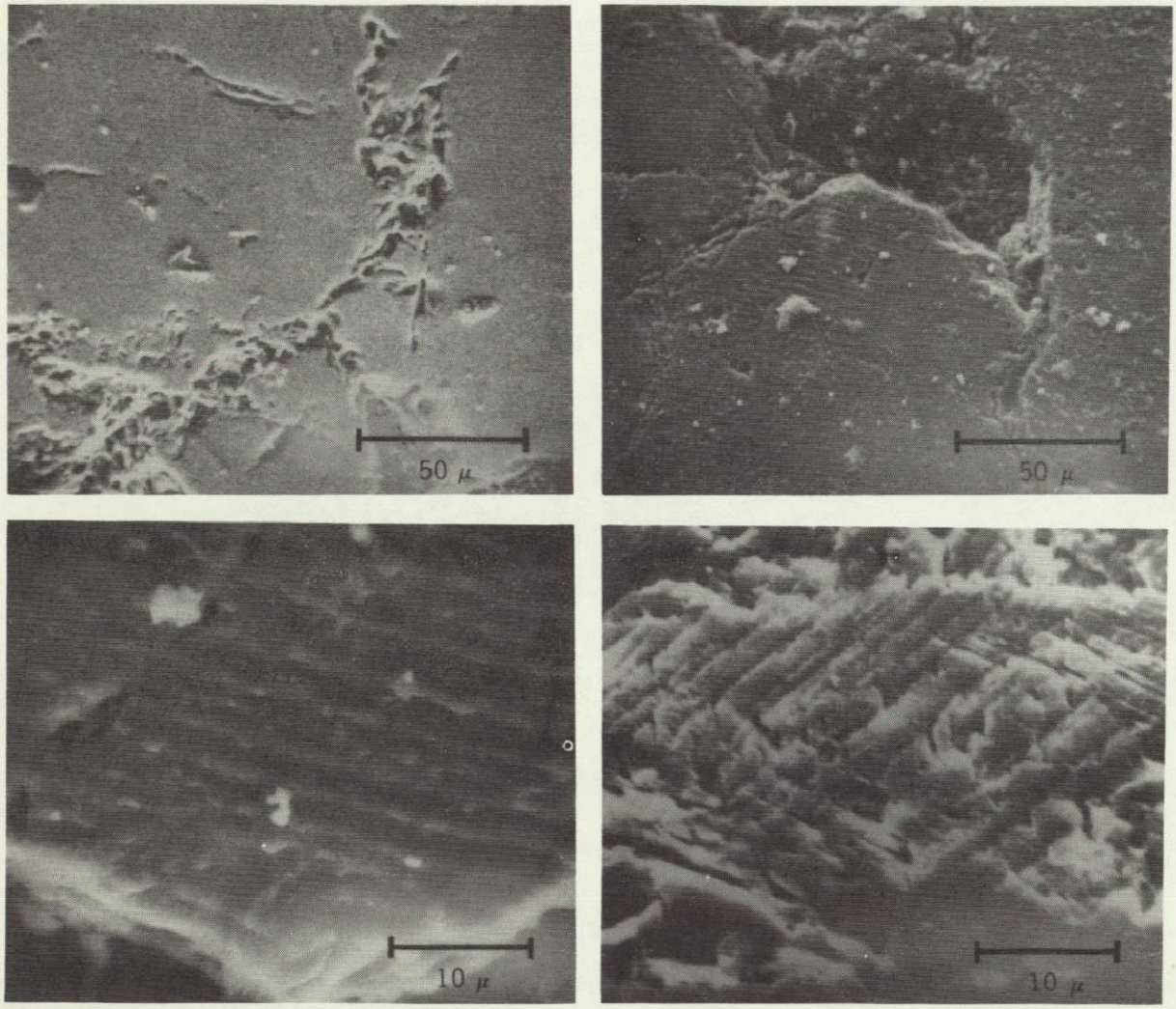

Plate 5. Planar features visible on a polished surface of 767-3, as seen by a scanning electron microscope. Upper left: unetched surface; no planar features evident. Upper right: a surface after a 5 second etch with 48% HF acid; some planar features now appear near center. Lower left: higher magnification view of planar features shown in upper right. Lower right: another surface, etched in HF for 60 seconds; two sets of planar features are now opened up by solution.

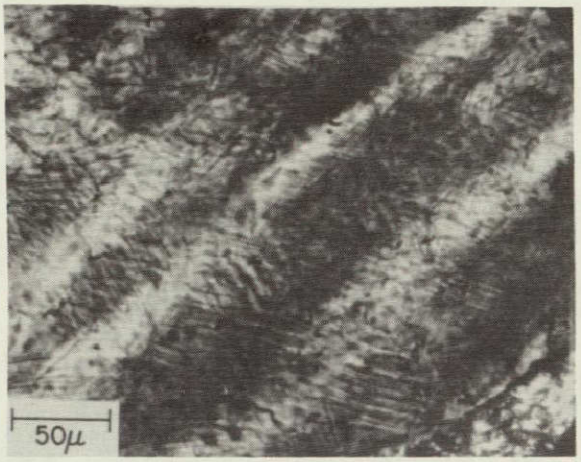

Plate 6(a). Detailed view of grid-twinned microline grain in 1067-47 showing several sets of planar features, some of which extend into adjacent twins. Crossed Nicols.

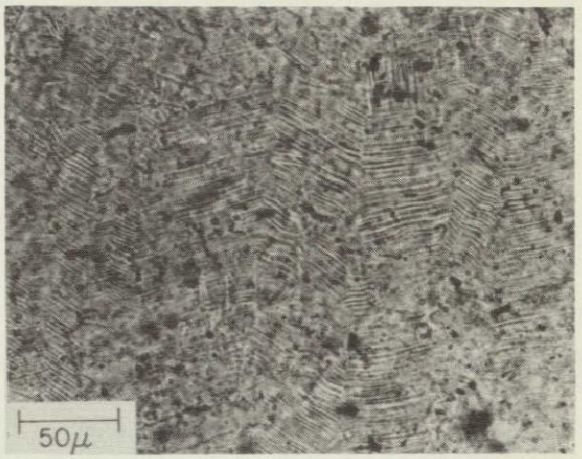

Plate 6(b). Part of a single plagioclase grain (Ab_{45}) in sample 767-4, photographed in plane-polarized light. The near vertical bands containing planar feature sets are alternate albite twins. The SW-trending planar features are oriented along (021) whereas the SE–trending sets, in alternate twins, follow (201) planes.

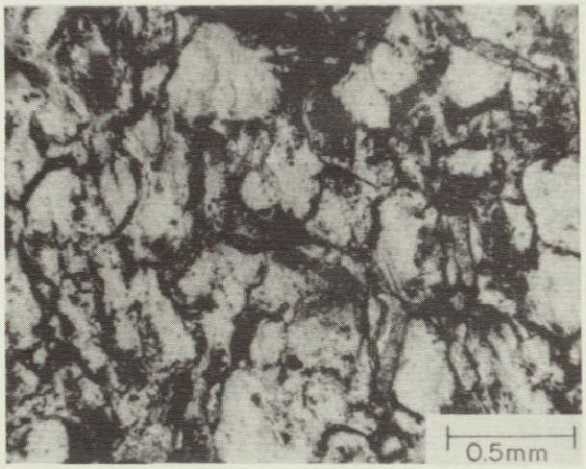

Plate 6(c). View of preserved quartzite texture in very strongly shocked sample 1067-94, as seen in uncrossed nicols. Individual grains retain their original outlines but have a "glassy" look. Dark areas within and between grains are melted matrix and/or tiny, coalesced bubbles (see Fig. 11).

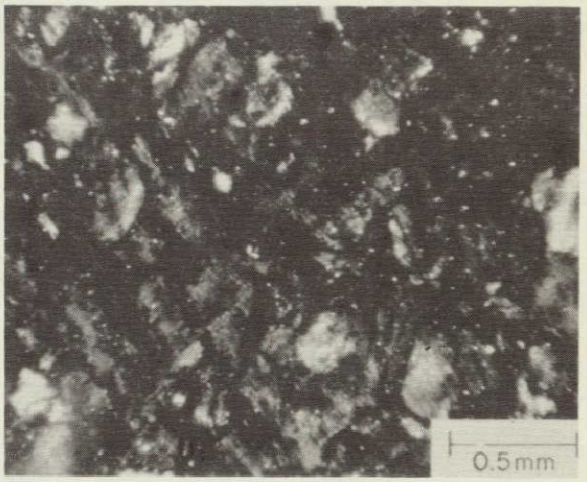

Plate 6(d). View of the same area of 1067-94 as shown in A, in cross-polarized light. Birefringence of most grains is notably reduced and a few grains have become isotropic. Small granular fragments and parts of individual grains still show near normal birefringence (bright spots).

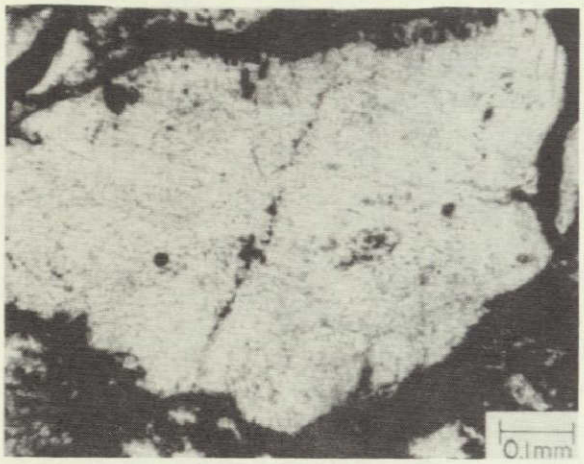

Plate 7(a). A grain in 767-5 composed of diaplectic glass derived from quartz, in which several sets of planar features are preserved. Uncrossed nicols (isotropic in cross-polarized light).

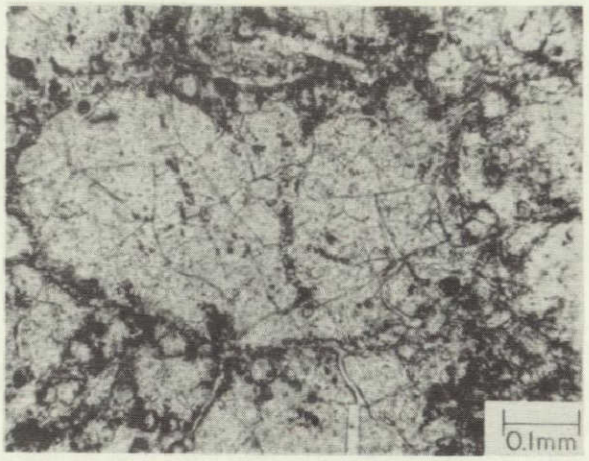

Plate 7(b). Quartz grains now converted to diaplectic glass, seen in plane-polarized light. Sample 1067-88. The irregular cracks running through several grains result from tensional stresses developed during cooling.

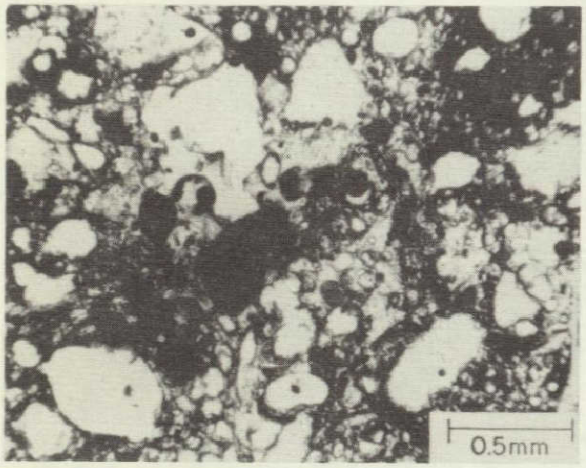

Plate 7(c). Characteristic microtexture of intensely shocked quartzite showing grains of diaplectic silica glass, numerous vesicles, fused matrix material, and incipient flow. Sample A-17. Uncrossed nicols.

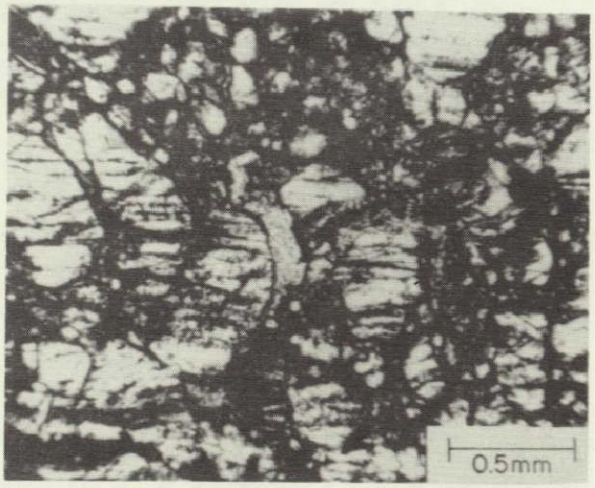

Plate 7(d). Grains of diaplectic silica glass in sample 1067-55. The dark, subparallel bands running through most grain areas are zones of incipient vesiculation. Uncrossed nicols.

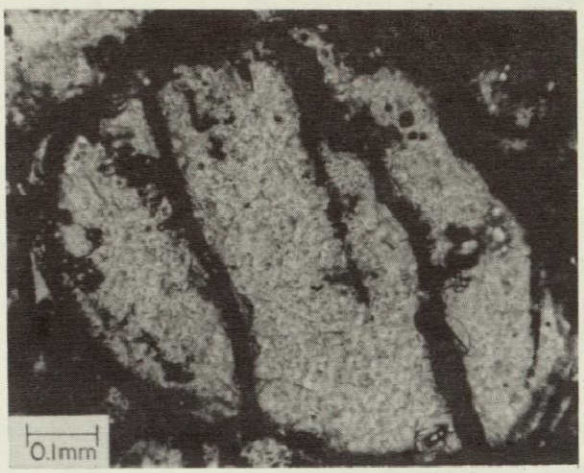

Plate 8(a). Single grain of diaplectic glass derived from quartz in sample A-6, showing several dark bands of tiny, coalesced bubbles. Note the irregular, minute cracks, similar to those commonly formed in rapidly cooled glasses. Nicols uncrossed.

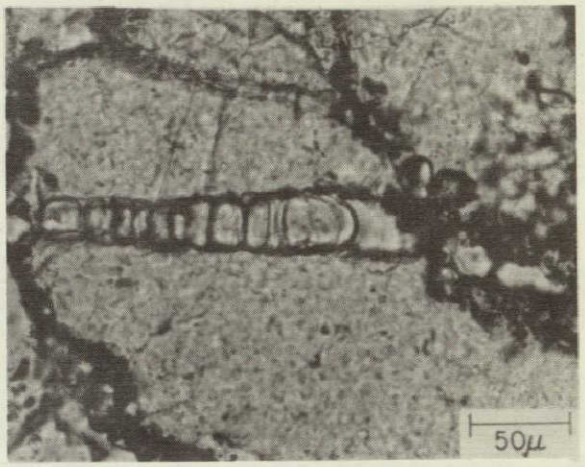

Plate 8(b). Detail of a single glassy grain in sample H-2, illustrating the effect of coalescing bubbles that produce the dark bands observed in many intensely shocked, vesiculated SEDAN quartzites. Uncrossed nicols.

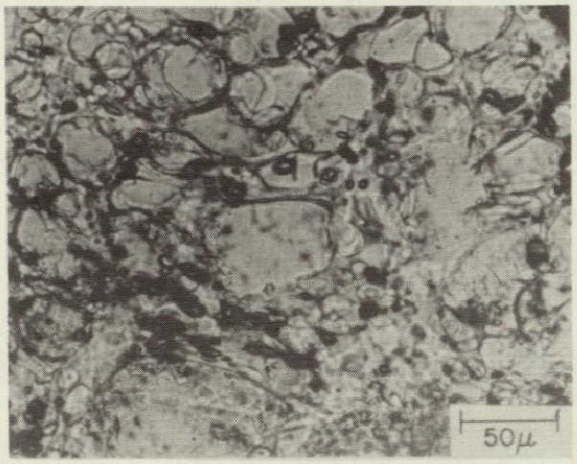

Plate 8(c). Intensely shocked quartzite (H-2) in which most quartz grains apparently melted and experienced some localized flow, as suggested in part by the small elongated bubble (lower center). Note the wide range of vesicle diameters. Nicols uncrossed.

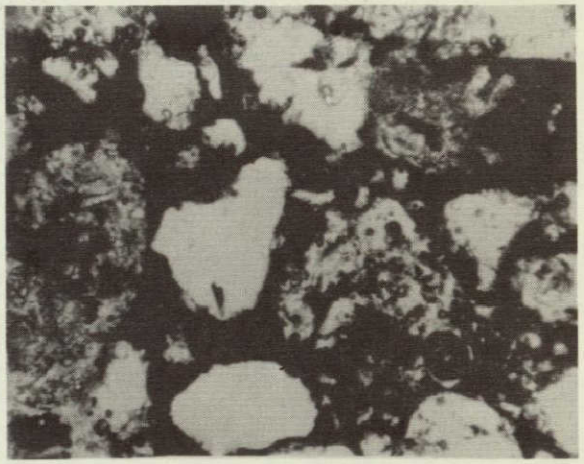

Plate 8(d). Region of sample 1067-93 containing dark brownish glass. This iron-rich glass occupies interstitial areas between diaplectic glass grains. Uncrossed nicols.

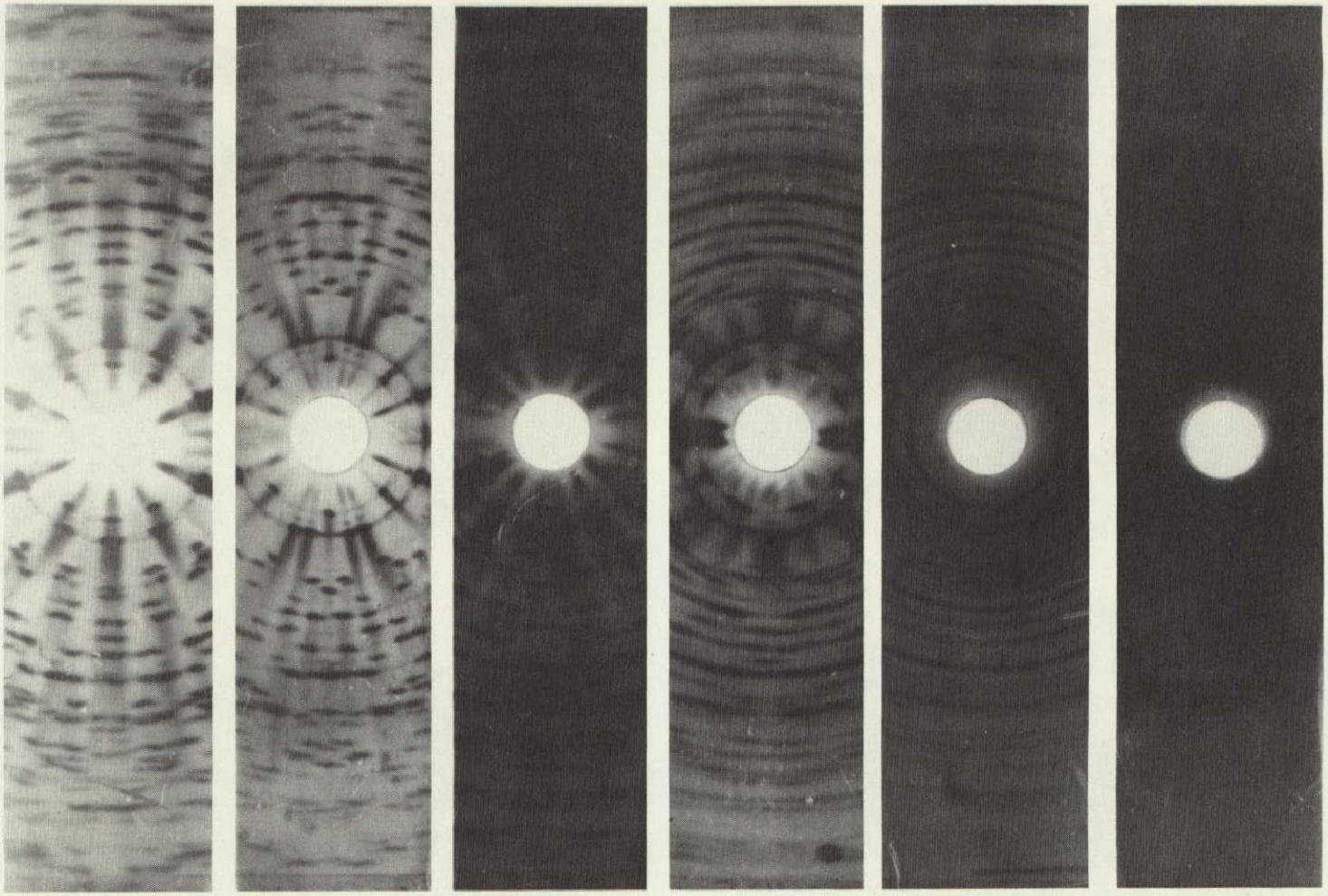

767–2 1067–65 A–19 767–6 A–6 A–8

Plate 9. Photographs of films showing diffraction patterns obtained from a quartz grain removed from each of six SEDAN samples listed at the bottom by using the x-ray asterism method described in text. Sample sequence, from left to right, is that of increasing shock damage as estimated from petrographic studies.

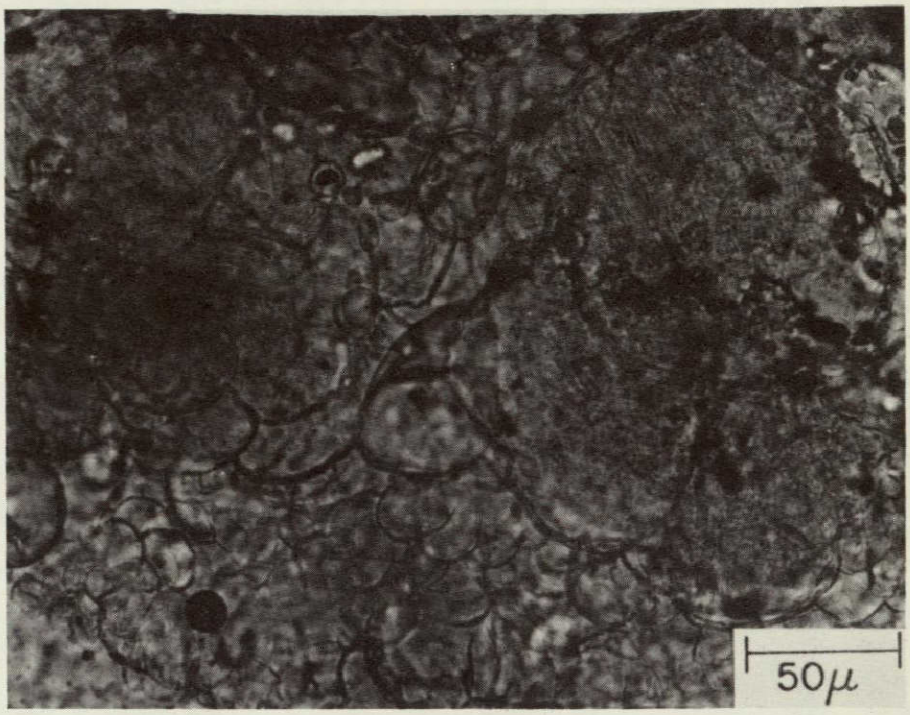

Plate 10(a). Example of unusual arcuate to ovoid microstructures formed in a single grain of diaplectic silica glass in a slab of sample 767-5 annealed for 24 hours at 1450° C. Thin section viewed in plane-polarized light, uncrossed nicols.

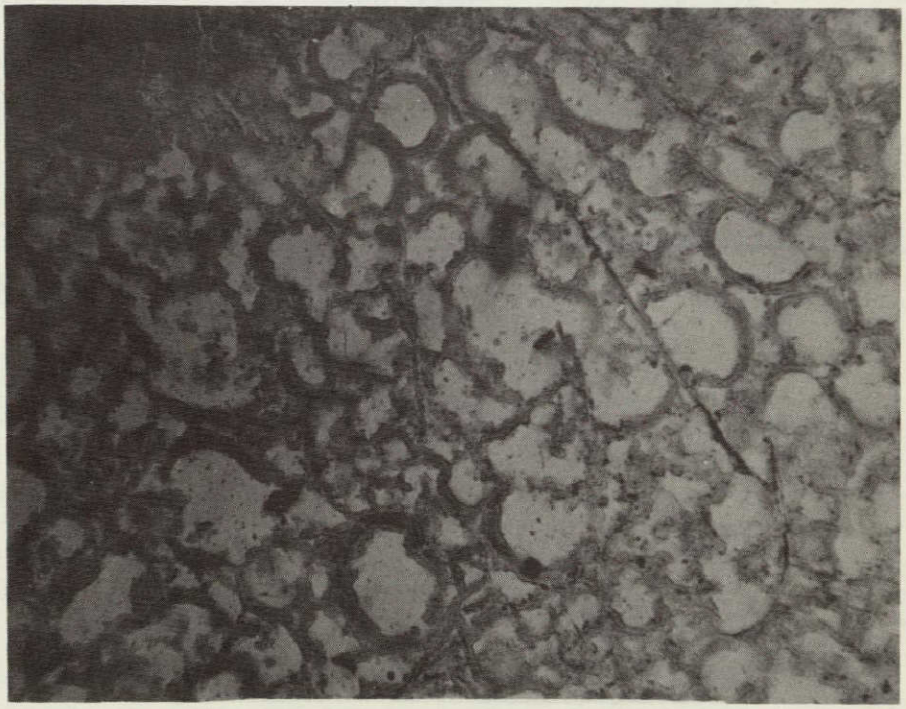

Plate 10(b). Ovoid microstructures present in a tectosilicate (quartz?) grain in a shocked granite gneiss from the Deep Bay, Canada impact structure. This feature may be similar in character and origin to the microstructures shown in a. Uncrossed nicols.

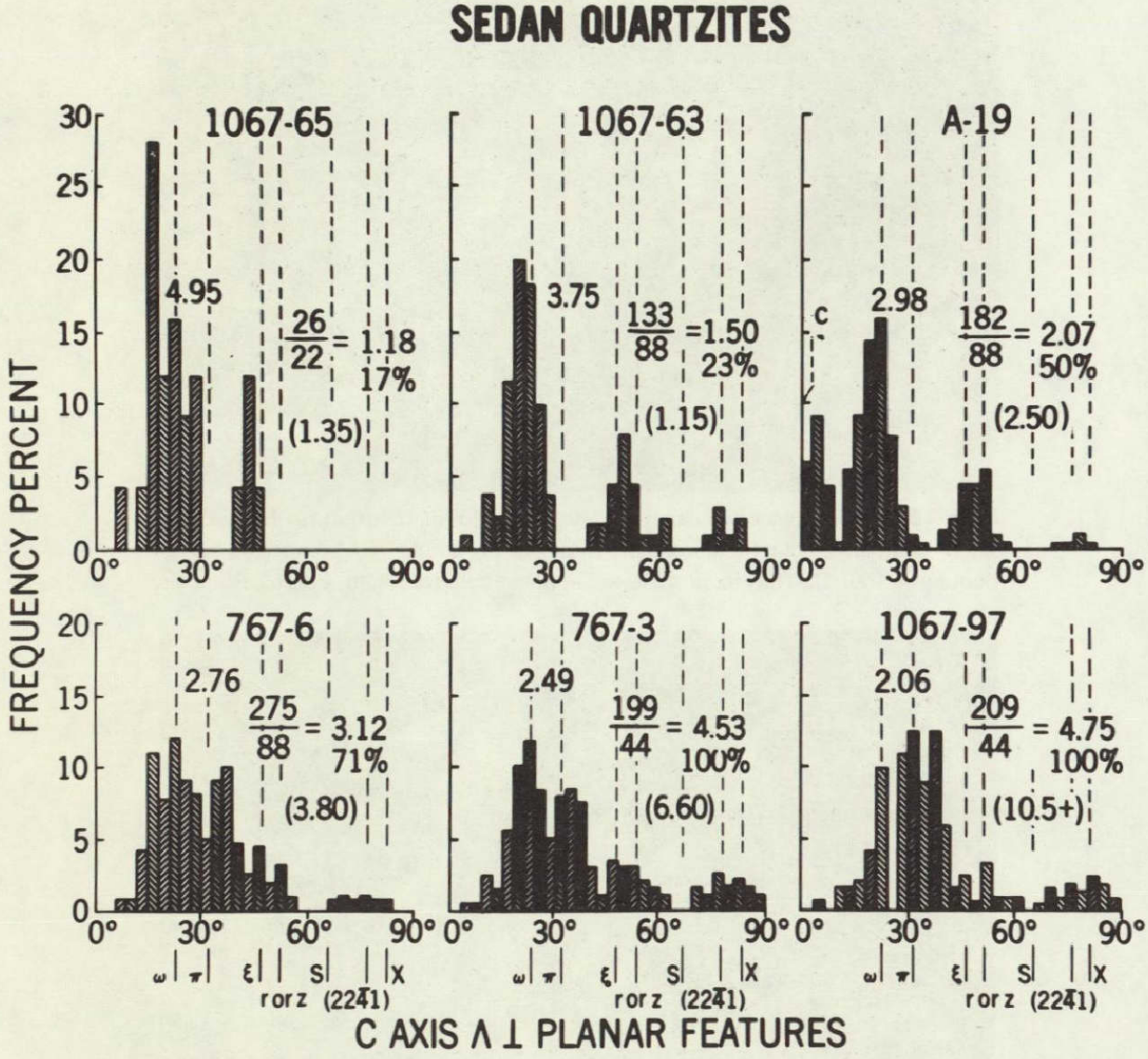

Figure 1. A series of histograms plotting the frequencies of angles between quartz c-axes and normals or poles to various planar feature sets in individual grains from six samples, arranged (upper left to lower right) in order of increasing shock damage. The numerical parameters associated with each histogram are explained in the text. Numbers in parenthesis are values obtained from x-ray asterism measurements (p. 43). Greek and arabic letters at indicated angles along lower abscissa row refer to specific crystallographic forms which plot at these angles.

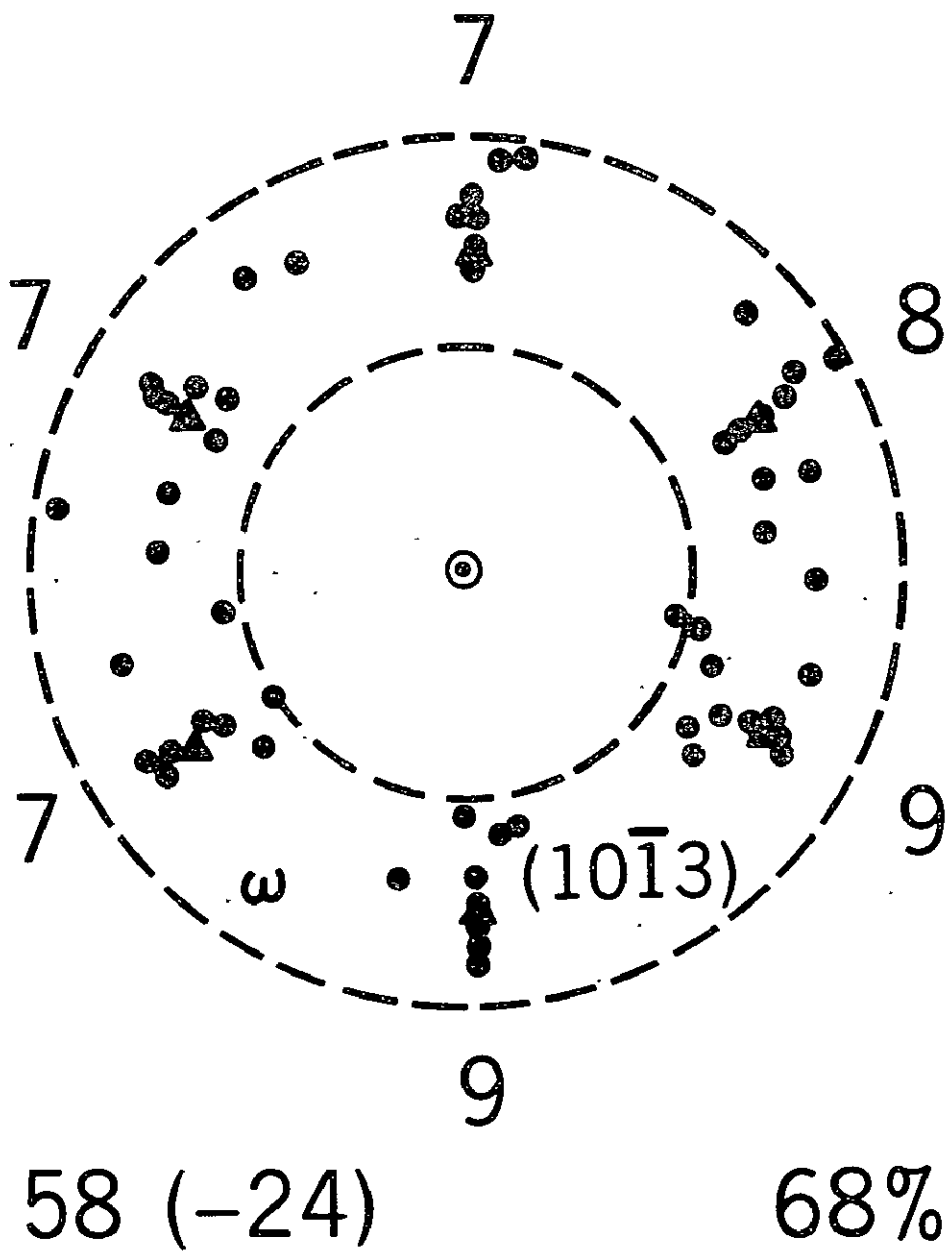

Figure 2. Stereonet plot of the orientation of measured poles to planar features sets with c-axis $\Lambda\perp$ set pole angles near 23° in sample 767-3. Poles shown as solid dots; all c-axes measurements were rotated to vertical on net (circled dot). Symmetry positions of the six planes of the crystal form $\omega\{10\bar{1}3\}$ are shown as triangles. See text for details of plotting procedure. Number 58 on lower left refers to total planar sets plotted whereas number 24 represents those planar sets from this total whose positions were arbitrarily plotted along radials containing the symmetry plane poles. Number located on the outer circumference along these radials denote all planar features (including those arbitrarily fixed) which lie within ±6° of their associated symmetry plane poles.

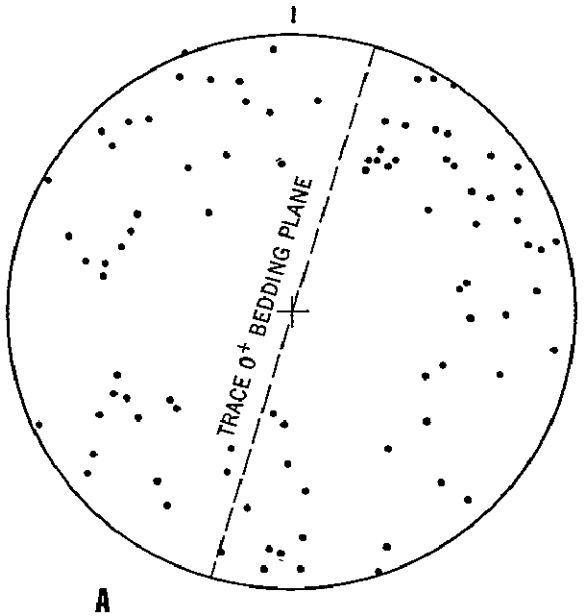

A

Figure 3.(a). Equal area lower hemisphere projection showing the orientation of c-axes for 72 quartz grains in sample 767-6;

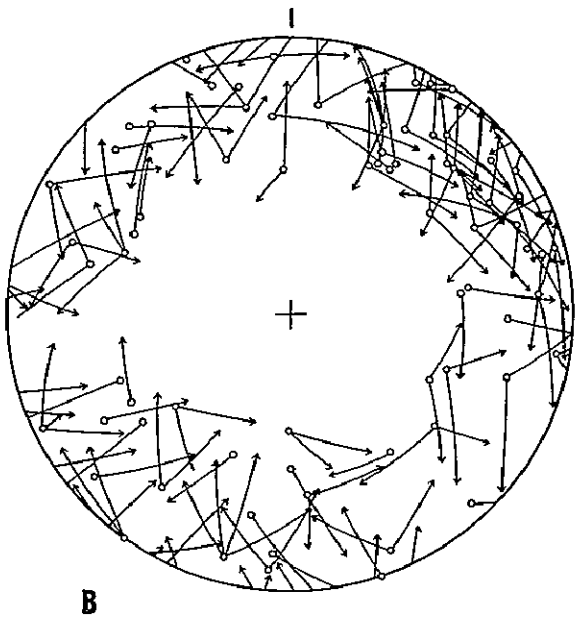

B

Figure 3(b). Poles to planar features (arrow-points) and the c-axis (open circles) of the same grain for 72 grains and 93 planar feature sets whose c-axis $\Lambda 1$ set angles lie in the 16° - 30° interval of Figure 1.

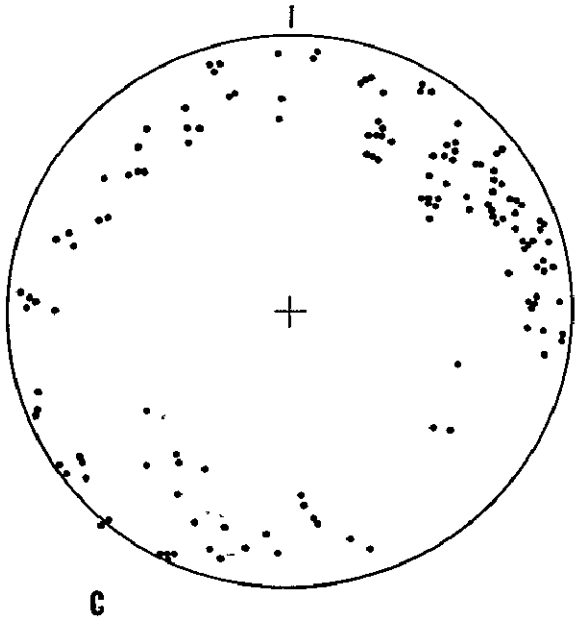

C

Figure 3(c). Plot of points representing intersections of arrow-tipped arcs shown in B;

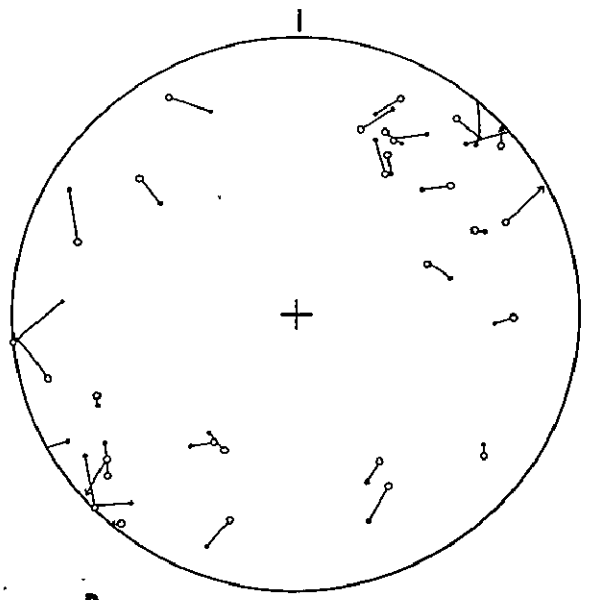

D

Figure 3(d). C-axes of the more (solid dots, c_2) and less (open circles, c_1) deformed parts of 30 quartz grains in 767-6. See text for details.

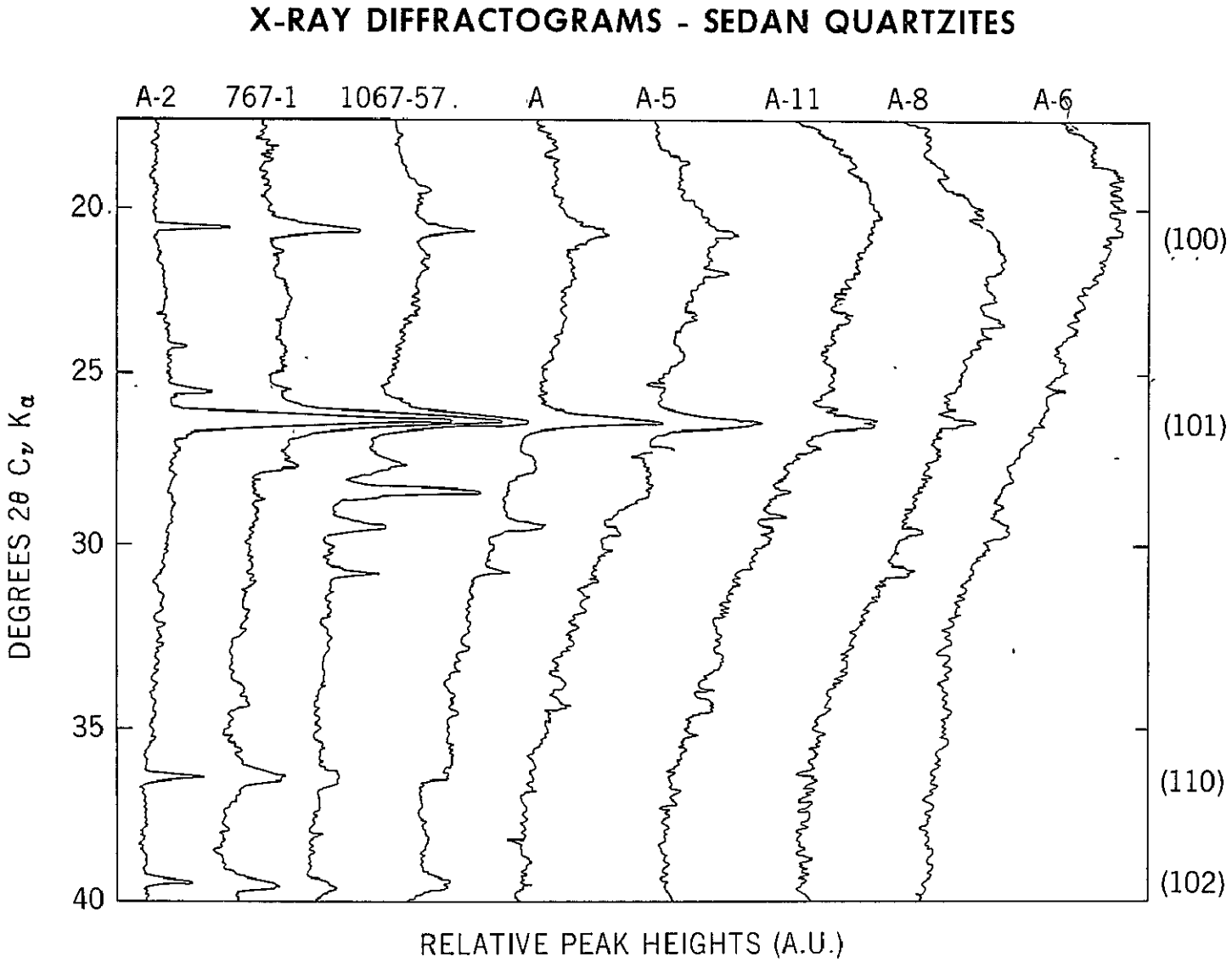

Figure 4. X-ray diffractograms made from powder mounts of eight SEDAN quartzite samples, arranged from left to right in order of increasing shock damage. Peaks near 20°, 27°, 36°, and 39° 2θ represent quartz reflection planes; those at 28°, 29°, and 31° are attributed to feldspars.

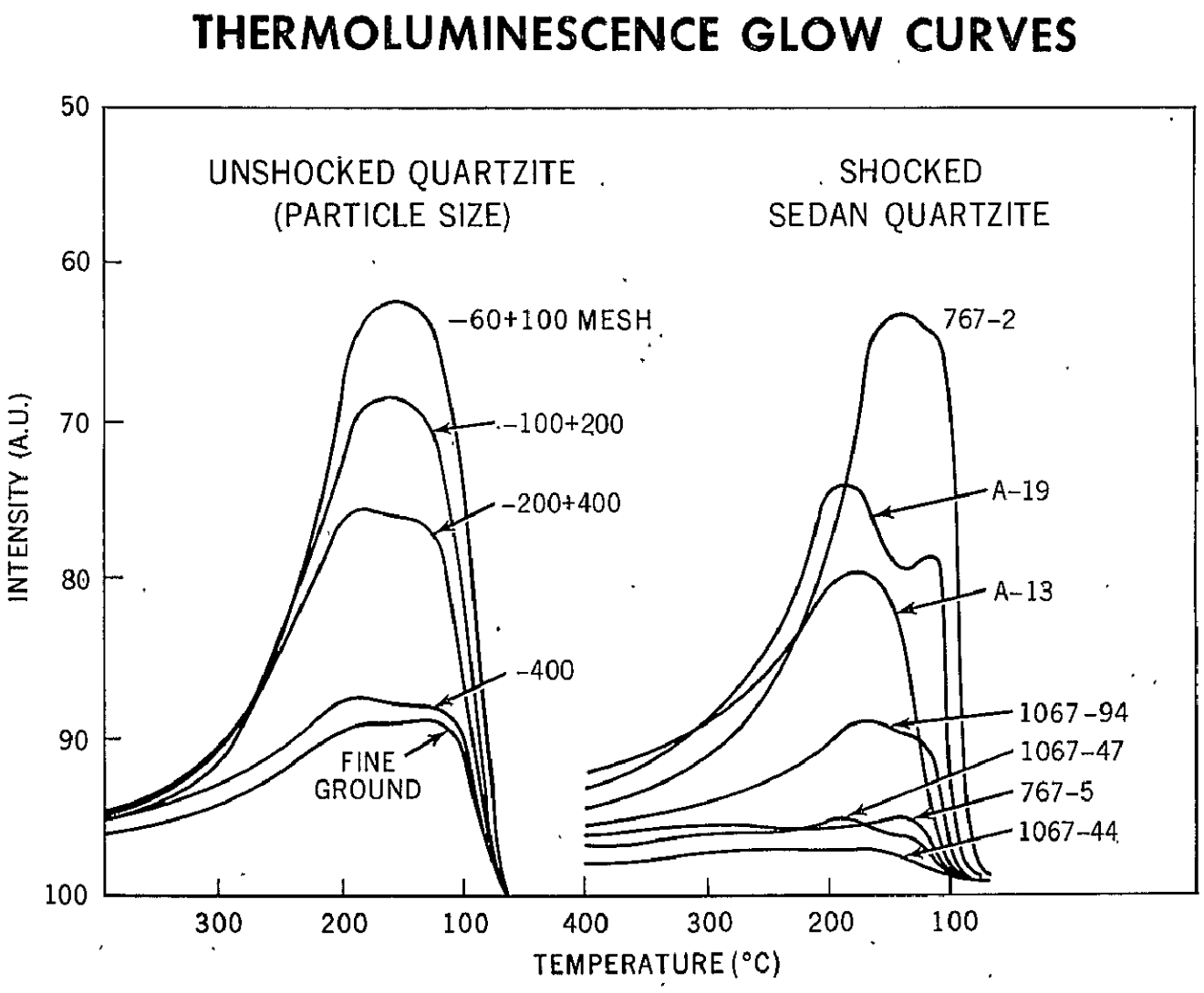

Figure 5. Thermoluminescence glow curves obtained by Dr. D. J. McDougall from a series of unshocked and shocked SEDAN quartzite samples. Curves on left were obtained from unshocked 767-2 which was ground up and sized to the mesh intervals shown. Curves on right result from runs on the -60 +100 mesh fractions of the different samples indicated. Sequence of decreasing peak heights is essentially that of increasing shock damage. See text.